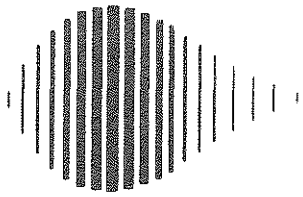

NATIONAL CENTER FOR EARTHQUAKE
ENGINEERING RESEARCH
State University of New York at Buffalo

SOLUTION OF THE DAM-RESERVOIR INTERACTION PROBLEM USING A COMBINATION OF FEM, BEM WITH PARTICULAR INTEGRALS, MODAL ANALYSIS AND SUBSTRUCTURING

by

C-S Tsai, G.C. Lee and R.L. Ketter
Department of Civil Engineering
State University of New York at Buffalo
Buffalo, NY 14260

Technical Report NCEER-88-0036

December 31, 1988

This research was conducted at the State University of New York at Buffalo and was partially supported by the National Science Foundation under Grant No. ECE 86-07591.

NOTICE

This report was prepared by the State University of New York at Buffalo as a result of research sponsored by the National Center for Earthquake Engineering Research (NCEER) and the National Science Foundation. Neither NCEER, associates of NCEER, its sponsors, State University of New York at Buffalo, nor any person acting on their behalf:

a. makes any warranty, express or implied, with respect to the use of any information, apparatus, method, or process disclosed in this report or that such use may not infringe upon privately owned rights; or

b. assumes any liabilities of whatsoever kind with respect to the use of, or the damage resulting from the use of, any information, apparatus, method or process disclosed in this report.

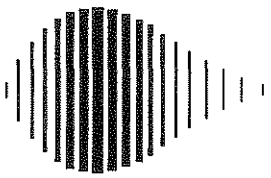

SOLUTION OF THE DAM-RESERVOIR INTERACTION PROBLEM USING A COMBINATION OF FEM, BEM WITH PARTICULAR INTEGRALS, MODAL ANALYSIS AND SUBSTRUCTURING

by

Chong-Shien Tsai[1], G.C. Lee[2] and R.L. Ketter[3]

December 31, 1988

Technical Report NCEER-88-0036

NCEER Contract Number 88-3017

NSF Master Contract Number ECE 86-07591

1 Research Associate, State University of New York at Buffalo
2 Dean and Professor of Civil Engineering, State University of New York at Buffalo
3 Director, National Center for Earthquake Engineering Research, and Leading Professor of Engineering and Applied Sciences, State University of New York at Buffalo

NATIONAL CENTER FOR EARTHQUAKE ENGINEERING RESEARCH
State University of New York at Buffalo
Red Jacket Quadrangle, Buffalo, NY, 14261

PREFACE

The National Center for Earthquake Engineering Research (NCEER) is devoted to the expansion and dissemination of knowledge about earthquakes, the improvement of earthquake-resistant design, and the implementation of seismic hazard mitigation procedures to minimize loss of lives and property. The emphasis is on structures and lifelines that are found in zones of moderate to high seismicity throughout the United States.

NCEER's research is being carried out in an integrated and coordinated manner following a structured program. The current research program comprises four main areas:

- Existing and New Structures
- Secondary and Protective Systems
- Lifeline Systems
- Disaster Research and Planning

This technical report pertains to Program 3, Lifeline Systems, and more specifically to the study of dams, bridges and infrastructures.

The safe and serviceable operation of lifeline systems such as gas, electricity, oil, water, communication and transportation networks, immediately after a severe earthquake, is of crucial importance to the welfare of the general public, and to the mitigation of seismic hazards upon society at large. The long-term goals of the lifeline study are to evaluate the seismic performance of lifeline systems in general, and to recommend measures for mitigating the societal risk arising from their failures.

In addition to the study of specific lifeline systems, such as water delivery and crude oil transmission systems, effort is directed toward the study of the behavior of dams, bridges and infrastructures under seismic conditions. Seismological and geotechnical issues, such as variation in seismic intensity from attenuation effects, faulting, liquefaction and spatial variability of soil properties are topics under investigation. These topics are shown in the figure below.

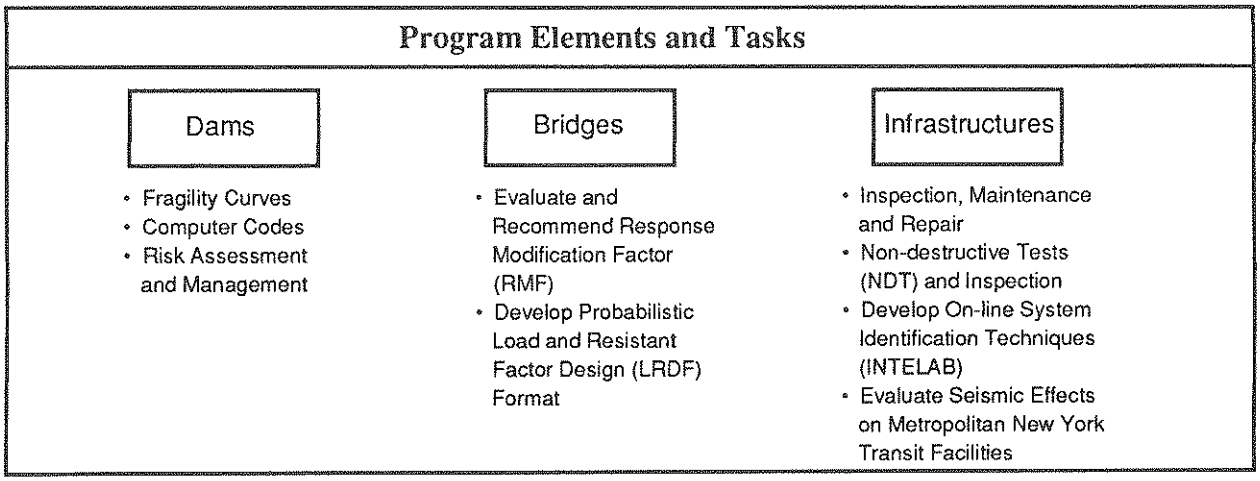

The authors have developed a method to describe the interaction between a reservoir and a dam structure. The method combines Finite Element Method (FEM), Boundary Element Method (BEM) with particular integrals, modal analysis, and substructuring techniques to derive this new analysis procedure. The procedure simplifies current analysis techniques and eliminates the need to recalculate the properties of the dam when the water level changes.

ABSTRACT

This report presents a new analysis procedure, which is a combination of the finite element method (FEM), the boundary element method (BEM) with particular integrals, modal analysis and substructuring. The difficulty of the nonsymmetric matrix generally introduced from the boundary element method with nonsymmetric and full matrix at the interface between the finite element and the boundary element methods is overcome by using the described procedure. A new boundary integral equation, which adopts a frequency-independent fundamental solution, is derived for solving the scalar wave equation.

Modal analysis of the dam without the reservoir is first addressed. Then, the modal added-mass and added-loads are calculated by using the boundary element method with particular integrals to solve the Helmholtz equation along with the boundary conditions, which are functions of modal shapes and generalized coordinates. After obtaining the modal added-mass and added-loads, the dam-reservoir system can be reformed in terms of modal shapes - with the reservoir empty - to obtain the natural frequencies, modal shapes, and response of the total system. Using this procedure, not only can the number of degrees-of-freedom of the nonsymmetric, full matrix be significantly reduced, but there is no need to recalculate the properties of the dam without the reservoir when the level of the water changes.

TABLE OF CONTENTS

SECTION	TITLE	PAGE
1	INTRODUCTION	1-1
2	THE DAM SUBSTRUCTURE SYSTEM	2-1
3	THE NEAR FIELD OF THE FLUID DOMAIN	3-1
4	PARTICULAR INTEGRALS IN TWO-DIMENSIONAL PROBLEMS	4-1
5	THE FAR FIELD OF THE INFINITE FLUID DOMAIN	5-1
6	THE GOVERNING EQUATIONS FOR THE DAM-RESERVOIR SYSTEM	6-1
7	NUMERICAL EXAMPLES	7-1
8	CONCLUSIONS	8-1
9	REFERENCES	9-1

LIST OF FIGURES

FIGURE	TITLE	PAGE
1-1	The Two-Dimensional Dam-Reservoir System	1-3
1-2	The Dam Body and the Reservoir Substructures	1-3
1-3	Division of the Fluid Domain Two Fields	1-4
7-1	Boundary Element Mesh of the Dam with Sloping Angle, $\theta = 10^{\circ}$	7-3
7-2	Hydrodynamic Pressures (Real Parts) Acting on the Dam with Sloping Angle $\theta = 10^{\circ}$ and with Frequency $\Omega = 1.5$. Results Are Almost Identical for Different Number of Interior Points	7-4
7-3	Hydrodynamic Pressures (Real Parts) Acting on the Dam with Sloping Angle, $\theta = 10^{\circ}$ and with Frequency $\Omega = 3.0$. Results Are Almost Identical for Different Number of Interior Points	7-5
7-4	Hydrodynamic Pressures (Imaginary Parts) Acting on the Dam with Sloping Angle $\theta = 10^{\circ}$ and with Frequency $\Omega = 3.0$. Results Are Almost Identical for Different Number of Interior Points	7-6
7-5	Hydrodynamic Pressures (Real Parts) Acting on the Dam with Sloping Angle, $\theta = 10^{\circ}$, and with Frequency $\Omega = 6.0$	7-7
7-6	Hydrodynamic Pressures (Imaginary Parts) Acting on the Dam with Sloping Angle, $\theta = 10^{\circ}$, and with Frequency $\Omega = 6.0$	7-8
7-7	Finite Element Mesh of the Reservoir for the Dam with Sloping Angle $\theta = 10^{\circ}$	7-9
7-8	Hydrodynamic Pressures (Real Parts) Acting on the Dam with Sloping Angle, $\theta = 10^{\circ}$: Comparison of Results Between the Proposed Method and the Finite Element Method	7-10
7-9	Hydrodynamic Pressures (Real Parts) Acting on the Dam with Sloping Angle, $\theta = 10^{\circ}$: Comparison of Results Between the Proposed Method and the Finite Element Method	7-11
7-10	Hydrodynamic Pressures (Imaginary Parts) Acting on the Dam with Sloping Angle, $\theta = 10^{\circ}$: Comparison of Results Between the Proposed Method and the Finite Element Method	7-12
7-11	The Dam-Reservoir System of Example 2	7-13
7-12	The Finite Element Mesh of the Dam Structure and the Boundary Element Mesh of the Near Field of the Fluid Domain in Example 2	7-14
7-13	The First Mode Shape of the Dam Without Water in Example 2 Natural Frequency = 4.069 Hz	7-15
7-14	The Second Mode Shape of the Dam Without Water in Example 2 Natural Frequency = 9.249 Hz	7-16

LIST OF FIGURES (Continued)

FIGURE	TITLE	PAGE
7-15	The Third Mode Shape of the Dam Without Water in Example 2 Natural Frequency = 10.95 Hz	7-17
7-16	The Fourth Mode Shape of the Dam Without Water in Example 2 Natural Frequency = 16.57 Hz	7-18
7-17	The Fifth Mode Shape of the Dam Without Water in Example 2 Natural Frequency = 23.67 Hz	7-19
7-18	The Sixth Mode Shape of the Dam Without Water in Example 2 Natural Frequency = 24.63 Hz	7-20
7-19	Frequency Response of the Dam of Example 2 Due to Horizontal Ground Motion	7-21

SECTION 1
INTRODUCTION

In the design of dams, especially for those in regions of active seismicity, the interaction between the reservoir and the dam structure is an important factor to take into account.

Hydrodynamic pressure distributions on dams subjected to seismic excitation was first developed by Westergaard[1] in 1933. Much research on this topic has been published since then. Zangar and Haefeli[2], Zienkiewicz and Nath[3], Chopra[4], Hanna and Humar[5] all treated the dam as a rigid body when establishing this distribution.

A number of methods have been proposed to ascertain the interaction of the structure and the fluid. Chopra and his co-workers[6],[7],[8] solved the problem using the finite element method for the structure and the continuum expression in the fluid domain. Further, the assumption was made that the face of the dam is vertical, and the floor of the reservoir extends flatly to infinity. Many authors have utilized the finite element method to model both the dam structure and the fluid domain. These include Saini, Bettess and Zienkiewicz[9], Hall and Chopra[10], Porter and Chopra[11], Kuo[12], Clough, Stephen and Kuo[13].

The boundary element method (BEM) is a powerful numerical tool for solving boundary value problems. For many cases, the BEM is more economical and accurate than are the finite difference and finite element methods. Tsai and Lee[14] used the combined FEM-BEM hybrid method to solve the dam-reservoir interaction problem. Tsai and Lee[15-17] utilized the BEM with particular integrals to address the dam-reservoir system phenomenon.

From an engineering point of view, the stress distribution in the dam body and the hydrodynamic pressure distribution on the face of the dam are of primary interest. Therefore, the finite element method (FEM) is frequently chosen to solve the dam problem; and the BEM is used for the fluid domain. The primary difficulty in following such a procedure is that the nonsymmetric and full matrix formulations of the BEM destroy the nicely banded and symmetry characteristics of the FEM.

Ohta, Kagawa and Honda[18] used the BEM and modal analysis techniques to analyze the fluid-structure vibration problem. In that study, the lumped added-mass and consistent added-mass are approximated, and the whole system equations are transformed into modal coordinates - from which the system natural frequencies and modal shapes are calculated.

In this report, a new procedure based on a combination of the FEM, BEM with particular intergrals, modal analysis and substructuring techniques will be derived. The dam body and fluid domain will be modeled using the FEM and BEM using particular integrals, respectively. First -

presuming the absence of water - modal analysis will be used to obtain natural frequencies and modal shapes of the dam. To obtain the modal added-mass and added-loads, the BEM with particular integrals will be used to solve the water wave equations, along with the boundary conditions which are functions of modal acceleration of the dam without water. After obtaining the modal added-mass and added-loads, the dam-reservoir system can be reformed in terms of modal shapes of the dam - with the reservoir empty - and the properties of the entire system can be calculated. Using this procedure, the entire system with the nonsymmetric full matrix can be reduced to a relatively small size set of calculations.

Quadratic elements and frequency-independent half space fundamental solutions, which satisfy the boundary condition at the free surface and increase the accuracy and save computer time, are used in the boundary element method. Radiation damping in the upstream direction of the reservoir is taken into account using a very simple procedure that will be described in the following section.

Dam-reservoir interaction analysis (see Fig. 1-1), based on the substructure concept, is presented in this report. Figure 1-2 shows the dam body and the reservoir substructures. The reservoir area can be divided into two fields; the near field -- close to the dam structure, and the far field - extending to infinity (see Fig. 1-3).

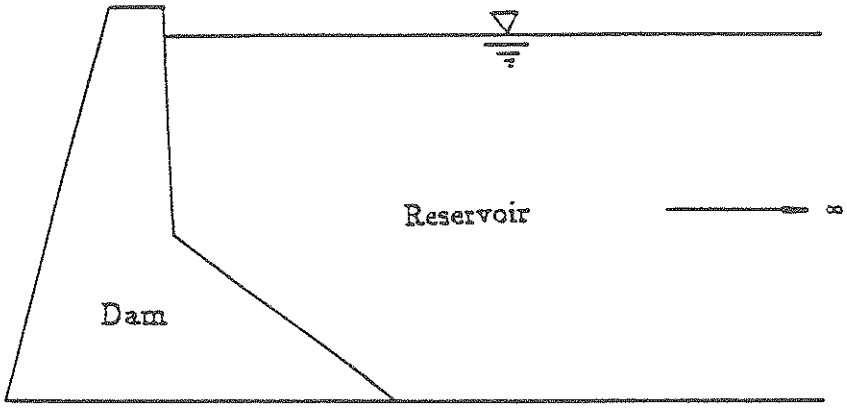

FIGURE 1-1 The Two-Dimensional Dam-Reservoir System

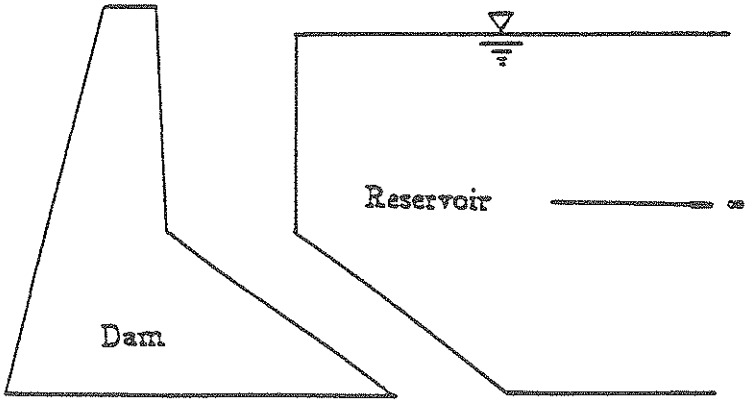

FIGURE 1-2 The Dam Body and the Reservoir Substructures

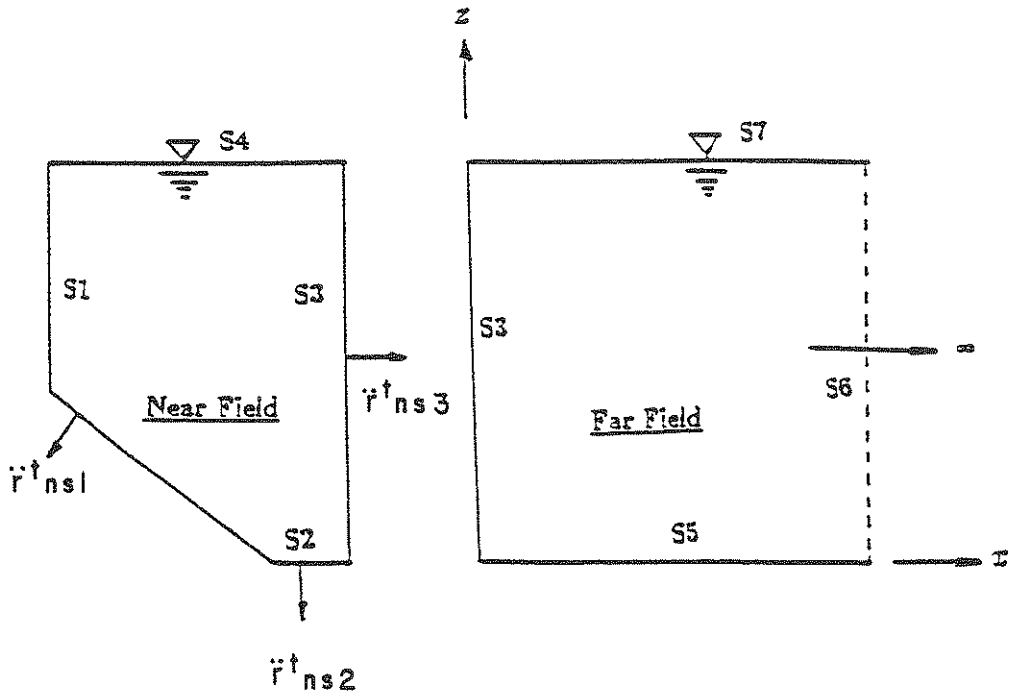

FIGURE 1-3 Division of the Fluid Domain Two Fields

SECTION 2
THE DAM SUBSTRUCTURE SYSTEM

Using the finite element method[19,20], the discretized equation of motion of the dam substructure can be expressed in the following form:

$$\underline{M}\,\ddot{\underline{V}}(t) + \underline{C}\,\dot{\underline{V}}(t) + \underline{K}\,\underline{V}(t) = -\underline{M}\,\underline{B}\,\ddot{u}_g(t) + \underline{F}(t) \qquad (2\text{-}1)$$

where:

$\ddot{\underline{V}}(t)$ = vector of nodal accelerations relative to ground,
$\dot{\underline{V}}(t)$ = vector of nodal velocities relative to ground,
$\underline{V}(t)$ = vector of nodal displacements relative to ground,
$\underline{M}$ = symmetric mass matrix of the finite element system of the dam structure,
$\underline{C}$ = symmetric damping maxtrix of the finite element system of the dam structure,
$\underline{K}$ = symmetric stiffness matrix of the finite element system of the dam structure,
$\ddot{u}_g(t)$ = vector of the ground acceleration,
$\underline{F}(t)$ = vector of hydrodynamic forces on the upstream face of the dam induced from the hydrodynamic pressure response of the reservoir, and
$\underline{B}$ = influence coefficient, each column of which expresses the total displacements of the dam resulting from a unit value of a boundary displacement.

The displacements of the dam, including hydrodynamic effects, can be approximately expressed as a linear combination of the first M modal shapes.

$$\underline{V}(t) = \sum_{m=1}^{M} \phi_m Y_m(t) \qquad (2\text{-}2)$$

The corresponding accelerations are

$$\ddot{\underline{V}}(t) = \sum_{m=1}^{M} \phi_m \ddot{Y}_m(t) \qquad (2\text{-}3)$$

Assuming that the damping matrix $\underline{C}$ is in a form which permits classical normal modes for the dam to be determined, equation (2-2) can be expressed as generalized displacements Y_m.

$$M_m^* \ddot{Y}_m(t) + C_m^* \dot{Y}_m(t) + K_m^* Y_m(t) = -\phi_m^T \underline{M}\,\underline{B}\,\ddot{u}_g(t) + F_m^*(t) \quad m = 1, 2, 3, \ldots, M \qquad (2\text{-}4)$$

The steady state responses to imposed harmonic ground accelerations $\ddot{u}_g(t) = E\,e^{i\omega t}$ would then be

$$\dot{Y}_m(t) = i\omega \overline{Y}_m(\omega)\, e^{i\omega t} \tag{2-5}$$

$$\ddot{Y}_m(t) = -\omega^2 \overline{Y}_m(\omega)\, e^{i\omega t} \tag{2-6}$$

$$F_m^*(t) = \overline{F}_m^*(\omega)\, e^{i\omega t} \tag{2-7}$$

and Equation (2-4) becomes

$$\left[-\omega^2 M_m^* + i\omega C_m^* + K_m^*\right] \overline{Y}_m(\omega) = -\phi_m^T \underline{M}\, \underline{B}\, \underline{E} + F_m^*(\omega) \qquad m = 1, 2, 3, \ldots, M \tag{2-8}$$

where

ϕ_m = the mth modal shape of the dam with empty reservoir,
$M_m^* = \phi_m^T \underline{M}\, \phi_m$ = generalized mass,
$C_m^* = \phi_m^T \underline{C}\, \phi_m = 2\zeta_m \omega_m M_m^*$ = generalized damping,
$K_m^* = \phi_m^T \underline{K}\, \phi_m = \omega_m^2 M_m^*$ = generalized stiffness,
$F_m^*(t) = \phi_m^T \underline{E}(t)$ = generalized load arising from the reservoir subjected to ground motions,
ζ_m = damping ratio of the mth mode,
ω_m = the frequency of the mth mode of the dam without the reservoir, and
ω = excitation frequencies.

SECTION 3
THE NEAR FIELD OF THE FLUID DOMAIN

Neglecting internal viscosity, and assuming the water to be linearly compressible, of small amplitude, and not subject to irrotational movement, the hydrodynamic pressure distribution in the reservoir is governed by the pressure wave equation

$$\nabla^2 P\,(x, z, t) = \frac{1}{C^2}\,\ddot{P}\,(x, z, t) \tag{3-1}$$

where

P(x,z,t) = hydrodynamic pressure distribution in excess of the hydrostatic pressure,
C = sonic velocity in water, and
x,z = Cartesian coordinates

The hydrodynamic pressure distribution can be obtained by solving Eq. (3-1), subject to the following boundary conditions (Fig. 1-3):

1. Surface S1 at the interface of the dam and the reservoir;

$$\frac{\partial P}{\partial n} = -\rho \ddot{r}^{t}_{ns1} \tag{3-2}$$

2. Surface S2 at the floor of the reservoir;

$$\frac{\partial P}{\partial n} = 0 \tag{3-3}$$

3. Surface S3 at the interface of the near field and the far field;

$$\frac{\partial P}{\partial n} = -\left(\frac{\partial P^*}{\partial n}\right) \tag{3-4}$$

$$P^* = P \tag{3-5}$$

4. Surface S4 at the free surface of the reservoir, if the surface wave is neglected.

$$P = 0 \tag{3-6}$$

where

n = the outward normal direction from the reservoir surface,
$\ddot{r}^t_{ns1}$ = the total normal acceleration of the surface in the fluid domain,
P^* = the hydrodynamic pressure at the interface of the near field and the far field, and
∂P^* = the normal derivative of the hydrodynamic pressure at the interface of the near field and the far field with respect to n.

The hydrodynamic pressure and its normal derivative are the sums of the complementary function and the particular integral. That is, the total solution [15-17] may be written in the following form:

$$P = P^c + P^p \tag{3-7}$$

and

$$\frac{\partial P}{\partial n} = \frac{\partial P^c}{\partial n} + \frac{\partial P^p}{\partial n} \tag{3-8}$$

The complementary function P^c satisfies

$$\nabla^2 P^c = 0 \tag{3-9}$$

with the particular integral P^p satisfying

$$\nabla^2 P^p = \frac{1}{C^2} \ddot{P} \tag{3-10}$$

The boundary integral equation for Eq. (3-9) is

$$\int_A \nabla^2 G(X, \xi) P^c(X) dA + \int_S G(X, \xi) \frac{\partial P^c}{\partial n}(X) dS - \int_S \frac{\partial G}{\partial n}(X, \xi) P^c(X) dS = 0 \tag{3-11}$$

Substituting Eqs. (3-7) and (3-8) into Eq. (3-11) yields

$$\begin{aligned} &\int_A (\nabla^2 G)\ P\, dA + \int_S G \frac{\partial P}{\partial n}\, dS - \int_S \frac{\partial G}{\partial n} P\, dS = \\ &\int_A (\nabla^2 G)\ P^p\, dA + \int_S G \frac{\partial P^p}{\partial n}\, dS - \int_S \frac{\partial G}{\partial n} P^p\, dS \end{aligned} \tag{3-12}$$

If the fundamental solution is chosen to satisfy

$$\nabla^2 G + \delta = 0 \tag{3-13}$$

and the boundary condition at the free surface

$$P = 0 \tag{3-14}$$

is met, then the frequency-independent fundamental solution is given by

$$G(X, \xi) = -\frac{1}{2\pi} \ln \frac{r}{r'} \tag{3-15}$$

Substituting Eqs. (3-13) and (3-14) into Eq. (3-12), the new boundary integral equation for the scaler wave equation is [15-17]

$$\begin{aligned} &C(\xi)P(\xi) + \int_{S\text{-}S4} G(X,\xi) \frac{\partial P}{\partial n}(X)dS - \int_{S\text{-}S4} \frac{\partial G}{\partial n}(X,\xi)P(X)dS \\ &= C(\xi)P^p(\xi) + \int_{S\text{-}S4} G(X,\xi) \frac{\partial P^p}{\partial n}(X)dS - \int_{S\text{-}S4} \frac{\partial G}{\partial n}(X,\xi)P^p(X)dS \end{aligned} \tag{3-16}$$

Equation (3-16) may be discretized in matrix form

$$\underline{H}\,\underline{P} - \underline{G}\left\{\frac{\partial P}{\partial n}\right\} = \underline{H}\,\underline{P}^p - \underline{G}\left\{\frac{\partial P^p}{\partial n}\right\} \tag{3-17}$$

In Eq. (3-17) the coefficients h_{ij} of the matrix $\underline{H}$ are

$$h_{ij} = \int_{\Delta S} \left(\frac{\partial G}{\partial n}\right)_{ij} N_j \, dS \quad \text{when } i \neq j \tag{3-18a}$$

and the coefficients g_{ij} of the matrix $\underline{G}$ are

$$g_{ij} = \int_{\Delta S} G_{ij} N_j \, dS \tag{3-18b}$$

where

ΔS = element length along the boundary surface,
G_{ij} = Green's function when the source point is at point i, and
N_j = shape function.

The strong singular term h_{ii} can be solved by a simple function which satisfies the governing equation [Eq. (3-9)] and the boundary condition at the free surface [15-17].

SECTION 4
PARTICULAR INTEGRALS IN TWO-DIMENSIONAL PROBLEMS

It is difficult to find particular integrals analytically when the geometry or the boundary conditions are complicated. Therefore, an approximation is introduced to obtain appropriate particular integrals. It is assumed that the hydrodynamic pressure distribution in the fluid domain may be approximated [15-17] by the expression

$$P(x, z, t) = \sum_{m=1}^{\infty} (r - r')_m \ \varphi_m(\xi, t) \tag{4-1}$$

Differentiation of this hydrodynamic pressure with respect to time is given by

$$\ddot{P}(x, z, t) = \sum_{m=1}^{\infty} (r - r')_m \ \ddot{\varphi}_m(\xi, t) \tag{4-2}$$

which, if the series is truncated into a finite number of terms, can be rewritten in matrix form.

$$\ddot{\underline{P}} = \underline{W} \ \ddot{\psi} \tag{4-3}$$

Substituting Eq. (4-2) into Eq. (3-10) yields

$$\nabla^2 P^p = \frac{1}{C^2} \sum_{m=1}^{\infty} (r - r')_m \ \ddot{\varphi}_m(\xi, t) \tag{4-4}$$

The particular integral satisfying Eq. (4-4) is

$$P^p = \frac{1}{C^2} \sum_{m=1}^{\infty} -\frac{1}{9}\left(r^3 - r'^3\right)_m \ \ddot{\varphi}_m(\xi, t) \tag{4-5}$$

Again truncating this series into a finite number of terms, Eq. (4-5) can be rewritten in the following matrix form

$$\underline{P}^p = \underline{D} \ \ddot{\psi} \tag{4-6}$$

The normal derivative of the particular integral would be given by

$$\frac{\partial P^p}{\partial n} = \frac{1}{C^2} \sum_{m=1}^{\infty} -\frac{1}{3} \left(r v_i n_i - r' v'_i n_i\right)_m \ddot{\varphi}_m(\xi, t) \tag{4-7}$$

In matrix form, this would be

$$\left\{\frac{\partial P^p}{\partial n}\right\} = \mathbf{T}\ddot{\psi} \tag{4-8}$$

where

$\varphi_m(\xi,t)$ = a fictitious density,
r = the distance between the source point and the field point,
r' = the distance between the image source point and the field point,
v_i = $(X-\xi)_i$, and
n_i = i component of the normal direction cosine.

After the particular integral and its normal derivative are obtained, they can be substituted into Eq. (3-17). This gives

$$\mathbf{H}\underline{P} - \mathbf{G}\left\{\frac{\partial P}{\partial n}\right\} = (\mathbf{H}\mathbf{D} - \mathbf{G}\mathbf{T})\ddot{\psi} \tag{4-9}$$

The differentiation of the fictitious density with respect to time, $\ddot{\psi}$, can be expressed as $\ddot{\underline{P}}$ from Eq. (4-3).

$$\ddot{\psi} = \mathbf{W}^{-1}\ddot{\underline{P}} \tag{4-10}$$

Substituting Eq. (4-10) into Eq. (4-9) yields

$$\mathbf{H}\underline{P} + \mathbf{M}\ddot{\underline{P}} = \mathbf{G}\left\{\frac{\partial P}{\partial n}\right\} \tag{4-11}$$

where

$$\mathbf{M} = (\mathbf{G}\mathbf{T} - \mathbf{H}\mathbf{D})\mathbf{W}^{-1} \tag{4-12}$$

Equation (4-11) can be solved as a classical dynamics problem.

Because the fundamental solution in Eq. (3-15) is only a function of a geometric condition along the source point, image source point, and field point, all frequency responses in Eq. (4-11) can be obtained by one integration.

SECTION 5
THE FAR FIELD OF THE INFINITE FLUID DOMAIN

If the reservoir in the upstream direction is considered large enough to be assumed as infinity, the effect of radiation damping in the modeling of an infinite fluid domain can be considered. In this analysis, the near field of the fluid domain is modeled by the boundary element method with particular integrals, while the far field is expressed as continuum expressions in the upstream direction.

The governing equation and boundary conditions of the far field are defined as follows: (see Fig. 1-3):

The governing equation is

$$\nabla^2 P(x, z, t) = \frac{1}{C^2} \ddot{P}(x, z, t) \tag{5-1}$$

1. Boundary condition on the surface S3;

$$\frac{\partial P}{\partial n} = -\left(\frac{\partial P^*}{\partial n}\right) \tag{5-2}$$

$$P^* = P \tag{5-3}$$

2. Boundary condition on surface S5;

$$\frac{\partial P}{\partial n} = 0 \tag{5-4}$$

3. Boundary condition on surface S6 (at infinity);

$$P = 0 \quad , \quad \text{and} \tag{5-5}$$

4. Boundary condition on the free surface S7;

$$P = 0 \tag{5-6}$$

When the dam-reservoir system is subjected to horizontal ground motion, the continuum solution for the steady state response at the interface of the near field and the far field of the fluid domain is governed by Eq. (5-7).

$$\bar{P}_{S3}(0, z, \omega) = \sum_{n=1}^{\infty} A_n \cos\lambda_n z \tag{5-7}$$

The normal derivative of the hydrodynamic pressure at the interface of the near field and far field is

$$\left(\frac{\partial \bar{P}}{\partial n}\right)_{S3}(0, z, \omega) = -\sum_{n=1}^{\infty} A_n \sqrt{\lambda_n^2 - \frac{\omega^2}{C^2}}\cos\lambda_n z \tag{5-8}$$

where

λ_n $= \dfrac{(2n-1)\pi}{2H}$
H = height of the reservoir, and
A_n = unknown coefficients.

From Eqs. (5-7) and (5-8), the following can be obtained:

$$\begin{aligned}\left(\frac{\partial \bar{P}}{\partial n}\right)_{S3}(0,z,\omega) &= -\frac{2}{H}\sum_{n=1}^{\infty}\sqrt{\lambda_n^2 - \frac{\omega^2}{C^2}}\left(\int_0^H \bar{P}_{S3}(0,z,\omega)\cos\lambda_n z\, dz\right)\cos\lambda_n z \\ &= -\frac{2}{H}\sum_{n=1}^{\infty}\sqrt{\lambda_n^2 - \frac{\omega^2}{C^2}}\left(\int_0^H \underline{N}_{S3}\cos\lambda_n z\, dz\right)\cos\lambda_n z\,\underline{\bar{P}}_{S3}\end{aligned} \tag{5-9}$$

In this equation, $\underline{N}_{S3}$ is the shape function along the interface of the near field and the far field of the fluid domain.

For the steady-state in the near field, Eq. (4-11) may be rewritten in the following matrix form:

$$\begin{bmatrix} H_{11} & H_{12} & H_{13} \\ H_{21} & H_{22} & H_{23} \\ H_{31} & H_{32} & H_{33} \end{bmatrix} \begin{Bmatrix} \underline{\bar{P}}_{S1} \\ \underline{\bar{P}}_{S2} \\ \underline{\bar{P}}_{S3} \end{Bmatrix} - \omega^2 \begin{bmatrix} M_{11} & M_{12} & M_{13} \\ M_{21} & M_{22} & M_{23} \\ M_{31} & M_{32} & M_{33} \end{bmatrix} \begin{Bmatrix} \underline{\bar{P}}_{S1} \\ \underline{\bar{P}}_{S2} \\ \underline{\bar{P}}_{S3} \end{Bmatrix}$$

$$= \begin{bmatrix} \underline{G}_{11} & \underline{G}_{12} & \underline{G}_{13} \\ \underline{G}_{21} & \underline{G}_{22} & \underline{G}_{23} \\ \underline{G}_{31} & \underline{G}_{32} & \underline{G}_{33} \end{bmatrix} \begin{Bmatrix} \left\{\frac{\partial \bar{P}}{\partial n}\right\}_{S1} \\ \left\{\frac{\partial \bar{P}}{\partial n}\right\}_{S2} \\ \left\{\frac{\partial \bar{P}}{\partial n}\right\}_{S3} \end{Bmatrix} = \begin{bmatrix} \underline{G}_{11} & \underline{G}_{12} \\ \underline{G}_{21} & \underline{G}_{22} \\ \underline{G}_{31} & \underline{G}_{32} \end{bmatrix} \begin{Bmatrix} \left\{\frac{\partial \bar{P}}{\partial n}\right\}_{S1} \\ \left\{\frac{\partial \bar{P}}{\partial n}\right\}_{S2} \end{Bmatrix} + \begin{bmatrix} \underline{G}_{13} \\ \underline{G}_{23} \\ \underline{G}_{33} \end{bmatrix} \left\{\frac{\partial \bar{P}}{\partial n}\right\}_{S3} \tag{5-10}$$

where

$\underline{\bar{P}}_{S1}$, $\underline{\bar{P}}_{S2}$, and $\underline{\bar{P}}_{S3}$, are hydrodynamic pressures at the surfaces S1, S2 and S3, respectively, and

$\left\{\frac{\partial \bar{P}}{\partial n}\right\}_{S1}$, $\left\{\frac{\partial \bar{P}}{\partial n}\right\}_{S2}$, and $\left\{\frac{\partial \bar{P}}{\partial n}\right\}_{S3}$, are the normal derivatives at the surfaces S1, S2 and S3, respectively.

The series in Eq. (5-9) may be rewritten in matrix form, if truncated to a finite number of terms.

$$\left\{\frac{\partial \bar{P}}{\partial n}\right\}_{S3} = R\,\underline{\bar{P}}_{S3} \tag{5-11}$$

where

$$R = -\frac{2}{H} \sum_{n=1}^{\infty} \sqrt{\lambda_n^2 - \frac{\omega^2}{C^2}} \left(\int_0^H \underline{N}_{S3} \cos\lambda_n z \, dz \right) \cos\lambda_n z \tag{5-12}$$

Substituting Eq. (5-11) into Eq. (5-10), the following set of equations is obtained

$$\begin{bmatrix} H_{11} & H_{12} & H_{13} \\ H_{21} & H_{22} & H_{23} \\ H_{31} & H_{32} & H_{33} \end{bmatrix} \begin{Bmatrix} \underline{\bar{P}}_{S1} \\ \underline{\bar{P}}_{S2} \\ \underline{\bar{P}}_{S3} \end{Bmatrix} - \omega^2 \begin{bmatrix} M_{11} & M_{12} & M_{13} \\ M_{21} & M_{22} & M_{23} \\ M_{31} & M_{32} & M_{33} \end{bmatrix} \begin{Bmatrix} \underline{\bar{P}}_{S1} \\ \underline{\bar{P}}_{S2} \\ \underline{\bar{P}}_{S3} \end{Bmatrix}$$

$$= \begin{bmatrix} \underline{G}_{11} & \underline{G}_{12} \\ \underline{G}_{21} & \underline{G}_{22} \\ \underline{G}_{31} & \underline{G}_{32} \end{bmatrix} \begin{Bmatrix} \left\{\frac{\partial \bar{P}}{\partial n}\right\}_{S1} \\ \left\{\frac{\partial \bar{P}}{\partial n}\right\}_{S2} \end{Bmatrix} + \begin{bmatrix} \underline{G}_{13} \\ \underline{G}_{23} \\ \underline{G}_{33} \end{bmatrix} \underline{R}\, \underline{\bar{P}}_{S3} \qquad (5\text{-}13)$$

Rearranging Eq. (5-13),

$$\begin{bmatrix} H_{11} & H_{12} & (H_{13} - \underline{G}_{13} \underline{R}) \\ H_{21} & H_{22} & (H_{23} - \underline{G}_{23} \underline{R}) \\ H_{31} & H_{32} & (H_{33} - \underline{G}_{33} \underline{R}) \end{bmatrix} \begin{Bmatrix} \underline{\bar{P}}_{S1} \\ \underline{\bar{P}}_{S2} \\ \underline{\bar{P}}_{S3} \end{Bmatrix} - \omega^2 \begin{bmatrix} M_{11} & M_{12} & M_{13} \\ M_{21} & M_{22} & M_{23} \\ M_{31} & M_{32} & M_{33} \end{bmatrix} \begin{Bmatrix} \underline{\bar{P}}_{S1} \\ \underline{\bar{P}}_{S2} \\ \underline{\bar{P}}_{S3} \end{Bmatrix}$$

$$= \begin{bmatrix} \underline{G}_{11} & \underline{G}_{12} \\ \underline{G}_{21} & \underline{G}_{22} \\ \underline{G}_{31} & \underline{G}_{32} \end{bmatrix} \begin{Bmatrix} \left\{\frac{\partial \bar{P}}{\partial n}\right\}_{S1} \\ \left\{\frac{\partial \bar{P}}{\partial n}\right\}_{S2} \end{Bmatrix} \qquad (5\text{-}14)$$

SECTION 6
THE GOVERNING EQUATIONS FOR THE DAM-RESERVOIR SYSTEM

The total acceleration $\overset{t}{\ddot{r}}_{ns1}(t)$ of the fluid particle at the interface of the dam structure and the fluid domain can be expressed as the relative acceleration $\underline{\ddot{Y}}_{S1}(t)$ at the upstream face of the dam and the ground motion $\ddot{u}_g(t)$.

$$\overset{t}{\ddot{r}}_{ns1} = -\Lambda \left[\underline{\ddot{Y}}_{S1}(t) + \underline{B}_{S1}\, \ddot{u}_g(t) \right] \tag{6-1}$$

From Eqs. (2-3), (3-2) and (6-1), the following equation can be obtained for steady state response cases,

$$\left\{ \frac{\partial \overline{P}(\omega)}{\partial n} \right\}_{S1} = -\rho\omega^2 \sum_{m=1}^{M} \Lambda \phi_{ms1}\, \overline{Y}_m(\omega) + \rho \Lambda \underline{B}_{S1}\, E \tag{6-2}$$

where

Λ, $\underline{B}_{S1}$ and ϕ_{ms1} are the direction cosine matrix, the influence matrix and the mode shape, respectively, along the interface of the dam and the fluid domain, and ρ = mass density of the fluid.

Substituting Eq. (6-2) into Eq. (5-14),

$$\begin{bmatrix} H_{11} & H_{12} & (H_{13} - G_{13} R) \\ H_{21} & H_{22} & (H_{23} - G_{23} R) \\ H_{31} & H_{32} & (H_{33} - G_{33} R) \end{bmatrix} \begin{Bmatrix} \underline{\overline{P}}_{S1} \\ \underline{\overline{P}}_{S2} \\ \underline{\overline{P}}_{S3} \end{Bmatrix} - \omega^2 \begin{bmatrix} M_{11} & M_{12} & M_{13} \\ M_{21} & M_{22} & M_{23} \\ M_{31} & M_{32} & M_{33} \end{bmatrix} \begin{Bmatrix} \underline{\overline{P}}_{S1} \\ \underline{\overline{P}}_{S2} \\ \underline{\overline{P}}_{S3} \end{Bmatrix}$$

$$= \begin{bmatrix} \underline{G}_{12} \\ \underline{G}_{22} \\ \underline{G}_{32} \end{bmatrix} \left\{ \frac{\partial \overline{P}}{\partial n} \right\}_{S2} - \rho\omega^2 \sum_{m=1}^{M} \begin{bmatrix} \underline{G}_{11} \\ \underline{G}_{21} \\ \underline{G}_{31} \end{bmatrix} \{ \Lambda \phi_{ms1} \}\, \overline{Y}_m(\omega) + \rho \begin{bmatrix} \underline{G}_{11} \\ \underline{G}_{21} \\ \underline{G}_{31} \end{bmatrix} \Lambda \underline{B}_{S1}\, \underline{E} \tag{6-3}$$

This can be expressed as

$$\begin{Bmatrix} \overline{\underline{P}}_{S1} \\ \overline{\underline{P}}_{S2} \\ \overline{\underline{P}}_{S3} \end{Bmatrix} = \begin{bmatrix} \underline{H}_{11} - \omega^2 \underline{M}_{11} & \underline{H}_{12} - \omega^2 \underline{M}_{12} & (\underline{H}_{13} - \underline{G}_{13} \underline{R} - \omega^2 \underline{M}_{13}) \\ \underline{H}_{21} - \omega^2 \underline{M}_{21} & \underline{H}_{22} - \omega^2 \underline{M}_{22} & (\underline{H}_{23} - \underline{G}_{23} \underline{R} - \omega^2 \underline{M}_{23}) \\ \underline{H}_{31} - \omega^2 \underline{M}_{31} & \underline{H}_{32} - \omega^2 \underline{M}_{32} & (\underline{H}_{33} - \underline{G}_{33} \underline{R} - \omega^2 \underline{M}_{33}) \end{bmatrix}^{-1}$$

$$\left(\begin{bmatrix} \underline{G}_{12} \\ \underline{G}_{22} \\ \underline{G}_{32} \end{bmatrix} \left\{ \frac{\partial \overline{P}}{\partial n} \right\}_{S2} - \rho\omega^2 \sum_{m=1}^{M} \begin{bmatrix} \underline{G}_{11} \\ \underline{G}_{21} \\ \underline{G}_{31} \end{bmatrix} \{\Lambda \phi_{ms1}\} \overline{Y}_m(\omega) + \rho \begin{bmatrix} \underline{G}_{11} \\ \underline{G}_{21} \\ \underline{G}_{31} \end{bmatrix} \Lambda \underline{B}_{S1} \underline{E} \right) \tag{6-4}$$

If the matrix $\underline{H}^*$ represents the inverse of the matrix in Eq. (6-4), the hydrodynamic pressure at the surface S1 is

$$\begin{aligned} \overline{\underline{P}}_{S1} = {} & [\underline{H}^*_{11} \ \underline{H}^*_{12} \ \underline{H}^*_{13}] \begin{bmatrix} \underline{G}_{12} \\ \underline{G}_{22} \\ \underline{G}_{32} \end{bmatrix} \left\{ \frac{\partial \overline{P}}{\partial n} \right\}_{S2} - \rho\omega^2 \ [\underline{H}^*_{11} \ \underline{H}^*_{12} \ \underline{H}^*_{13}] \begin{bmatrix} \underline{G}_{11} \\ \underline{G}_{21} \\ \underline{G}_{31} \end{bmatrix} \Lambda \Phi_{S1} \{\overline{Y}\,\omega)\} \\ & + \rho \ [\underline{H}^*_{11} \ \underline{H}^*_{12} \ \underline{H}^*_{13}] \begin{bmatrix} \underline{G}_{11} \\ \underline{G}_{21} \\ \underline{G}_{31} \end{bmatrix} \Lambda \underline{B}_{S1} \underline{E} \end{aligned} \tag{6-5}$$

where

Φ_{S1} = matrix of the finite modes of mode shapes along the surface S1, and
$\{Y(\omega)\}$ = vector of the finite terms of generalized coordinates.

Equation (6-5) can be rewritten in the following form:

$$\overline{\underline{P}}_{S1} = \underline{Q}_{ns2} \left\{ \frac{\partial P}{\partial n} \right\}_{S2} - \omega^2 \underline{Q}^M_{ns1} \{\overline{Y}\,\omega)\} + \underline{Q}^o_{ns1} \underline{B}_{S1} \underline{E} \tag{6-6}$$

where

$$\underline{Q}_{ns2} = [\underline{H}^*_{11} \ \underline{H}^*_{12} \ \underline{H}^*_{13}] \begin{bmatrix} \underline{G}_{12} \\ \underline{G}_{22} \\ \underline{G}_{32} \end{bmatrix} \tag{6-7}$$

$$\underline{Q}^M_{ns1} = \rho \ [\underline{H}^*_{11} \ \underline{H}^*_{12} \ \underline{H}^*_{13}] \begin{bmatrix} \underline{G}_{11} \\ \underline{G}_{21} \\ \underline{G}_{31} \end{bmatrix} \Lambda \Phi_{S1} \tag{6-8}$$

$$\underline{Q}^{o}_{ns1} = \rho \, [H^{*}_{11} \; H^{*}_{12} \; H^{*}_{13}] \begin{bmatrix} \underline{G}_{11} \\ \underline{G}_{21} \\ \underline{G}_{31} \end{bmatrix} \Lambda \tag{6-9}$$

Based on the virtual work principle, the equivalent nodal forces acting on the upstream face of the dam due to hydrodynamic pressures induced by ground motions are given by [14]

$$\overline{\underline{F}} = - \int_{S1} \varphi^{T}_{S1} \Lambda^{T} \overline{P}_{S1} \, dS = - \int_{S1} \varphi^{T}_{S1} \Lambda^{T} \underline{N}_{S1} \, dS \overline{\underline{P}}_{S1} = - \underline{S}_{ns1} \overline{\underline{P}}_{S1} \tag{6-10}$$

where

$\underline{S}_{ns1} = \int_{S1} \varphi^{T}_{S1} \Lambda^{T} \underline{N}_{S1} \, dS,$

φ_{S1} = shape function of the dam structure along the upstream surface, and

$\underline{N}_{S1}$ = shape function of the fluid domain along the interface of the dam and the fluid domain.

The equivalent nodal forces on the dam face induced from the hydrodynamic pressure are given by

$$\overline{\underline{F}} = - \underline{S}_{ns1} \overline{\underline{P}}_{S1} = - \underline{M}_{ns2} \left\{ \frac{\partial \overline{P}}{\partial n} \right\}_{S2} + \omega^{2} \underline{M}^{M}_{ns1} \, \{ \overline{Y}(\omega) \} - \underline{M}^{o}_{ns1} \underline{B}_{S1} \underline{E} \tag{6-11}$$

where

$$\underline{M}_{ns2} = \underline{S}_{ns1} \underline{Q}_{ns2} \tag{6-12}$$

$$\underline{M}^{M}_{ns1} = \underline{S}_{ns1} \underline{Q}^{M}_{ns1} \tag{6-13}$$

$$\underline{M}^{o}_{ns1} = \underline{S}_{ns1} \underline{Q}^{o}_{ns1} \tag{6-14}$$

The generalized force induced from the hydrodynamic effect is, then,

$$\overline{\underline{F}}^{*}_{m}(\omega) = \phi^{T}_{m} \overline{\underline{F}}(\omega) = - \phi^{T}_{m} \underline{M}_{ns2} \left\{ \frac{\partial \overline{P}}{\partial n} \right\}_{S2} + \omega^{2} \phi^{T}_{m} \underline{M}^{M}_{ns1} \, \{ \overline{Y}(\omega) \} - \phi^{T}_{m} \underline{M}^{o}_{ns1} \underline{B}_{S1} \underline{E} \tag{6-15}$$

Substituting Eq. (6-15) into Eq. (2-8), the equation may be rearranged in matrix form as follows:

$$\begin{bmatrix} m_{11} & m_{12} & \dots & m_{1M} \\ m_{21} & \dots & \dots & m_{2M} \\ \vdots & \ddots & \ddots & \vdots \\ m_{M1} & m_{M2} & \dots & m_{MM} \end{bmatrix} \begin{Bmatrix} \overline{Y}_1(\omega) \\ \overline{Y}_2(\omega) \\ \vdots \\ \overline{Y}_M(\omega) \end{Bmatrix} + \begin{bmatrix} i\omega C_1^* & 0 & \dots & 0 \\ 0 & i\omega C_2^* & \dots & 0 \\ \vdots & \ddots & \ddots & \vdots \\ 0 & 0 & \dots & i\omega C_M^* \end{bmatrix} \begin{Bmatrix} \overline{Y}_1(\omega) \\ \overline{Y}_2(\omega) \\ \vdots \\ \overline{Y}_M(\omega) \end{Bmatrix}$$

$$+ \begin{bmatrix} K_1^* & 0 & \dots & 0 \\ 0 & K_2^* & \dots & 0 \\ \vdots & \ddots & \ddots & \vdots \\ 0 & 0 & \dots & K_M^* \end{bmatrix} \begin{Bmatrix} \overline{Y}_1(\omega) \\ \overline{Y}_2(\omega) \\ \vdots \\ \overline{Y}_M(\omega) \end{Bmatrix} = \begin{Bmatrix} L_1(\omega) \\ L_2(\omega) \\ \vdots \\ L_M(\omega) \end{Bmatrix} \tag{6-16}$$

where

$$m_{jl}(\omega) = -\omega^2 \phi_j^T \underline{M}_{ns1}^l \quad j \neq 1 \tag{6-17}$$

$$m_{jj}(\omega) = -\omega^2 M_j^* - \omega^2 \phi_j^T \underline{M}_{ns1}^j \tag{6-18}$$

$$L_j(\omega) = -\phi_j^T (\underline{M} + \underline{M}_{ns1}^o)\, \underline{B}\, \underline{E} - \phi_j^T \underline{M}_{ns2} \left\{ \frac{\partial \overline{P}}{\partial n} \right\}_{S2} \tag{6-19}$$

Equation (6-16) may be rearranged and expressed in the following form:

$$\begin{bmatrix} A_{12} & A_{13} & \dots & A_{1M} \\ A_{21} & \dots & \dots & A_{2M} \\ \vdots & \ddots & \ddots & \vdots \\ A_{M1} & A_{M2} & \dots & A_{MM} \end{bmatrix} \begin{Bmatrix} \overline{Y}_1(\omega) \\ \overline{Y}_2(\omega) \\ \vdots \\ \overline{Y}_M(\omega) \end{Bmatrix} = \begin{Bmatrix} L_1(\omega) \\ L_2(\omega) \\ \vdots \\ L_M(\omega) \end{Bmatrix} \tag{6-20}$$

where

$$A_{jl}(\omega) = -\omega^2 \phi_j^T \underline{M}_{ns1}^l \quad j \neq 1 \tag{6-21}$$

$$A_{jj}(\omega) = \left[-\omega^2 M_j^* + i\omega C_j^* + K_j^* \right] - \omega^2 \phi_j^T \underline{M}_{ns1}^j \tag{6-22}$$

$$L_j(\omega) = -\phi_j^T (\underline{M} + \underline{M}_{ns1}^o)\, \underline{B}\, \underline{E} - \phi_j^T \underline{M}_{ns2} \left\{ \frac{\partial \overline{P}}{\partial n} \right\}_{S2} \tag{6-23}$$

and

$\underline{M}^{j}_{ns1}$ = the jth column vector of the matrix $\underline{M}^{M}_{ns1}$.

Once the complex frequency responses $Y(\omega)$, m=1,2,3,...,M are obtained from Eq. (6-20) for a range of values ω, the responses to arbitrary ground motions $\ddot{u}_g(t)$ can be obtained by Fourier synthesis of the responses to individual harmonic components.

$$Y_m(t) = \frac{1}{2\pi}\int_{-\infty}^{\infty} \overline{Y}_m(\omega)\ddot{u}_g(\omega)e^{i\omega t}\,d\omega \tag{6-24}$$

where $\ddot{u}_g(\omega)$ is the Fourier transform of $\ddot{u}_g(t)$,

$$\ddot{u}_g(\omega) = \int_0^{t_d} \ddot{u}_g(t)e^{-i\omega t}\,dt \tag{6-25}$$

and t_d = duration of the ground motion.

The nodal displacement $\underline{V}(t)$ can then be obtained from Eqs. (2-2) and (6-24).

In general, for infinite reservoirs, the matrices $\underline{M}^{o}_{ns1}$, $\underline{M}^{M}_{ns1}$, and $\underline{M}_{ns2}$ are complex valued and dependent upon the excitation frequency due to the matrices $\underline{R}$ in Eqs. (5-14) and (6-4), which represent the radiation boundary condition along the interface of the near field and the far field of the fluid domain. They introduce additional damping in the dam-reservoir system. However, if water compressibility is neglected, those terms will be real valued.

For finite reservoirs, $\phi_j^T \underline{M}^{l}_{ns1}$ is the added-mass term, which is real valued, and has an influence on the basic behavior of the dam-reservoir system. $-\phi_j^T M^{o}_{ns1} B_{S1} E - \phi_j^T \underline{M}_{ns2}\left\{\frac{\partial \overline{P}}{\partial n}\right\}_{S2} - \phi_j^T M_{ns3}\left\{\frac{\partial \overline{P}}{\partial n}\right\}_{S3}$ are added-loads which are real valued, and represent the additional external loads associated with accelerations on the surfaces S1, S2 and S3, respectively. The added-mass matrix is full and nonsymmetric. Its size may be reduced, and is a function of the number of modes taken. The nonsymmetric characteristic is due to the nonsymmetric characteristic of the boundary element method. The matrix of the dam-reservoir system is a full matrix because the modal shape of the dam without water does not allow decoupling of the entire dam-reservoir system.

The added-load terms $\Phi_j^T M^{o}_{ns1} B_{S1} E$ are associated with the hydrodynamic pressures acting on the dam face due to ground motions when the dam is assumed to be rigid. If the compressibility of the water is neglected, the modal added-mass and added-load are frequency-independent.

SECTION 7
NUMERICAL EXAMPLES

To demonstrate the accuracy and feasibility of the proposed method, consider the following examples:

Example 1: Hydrodynamic Pressures on Sloping Dams with Infinite Reservoir

In this example, the hydrodynamic pressures on rigid dams having upstream faces with sloping angle $\theta = 10^{o}$ are examined. The discretized boundary element mesh is shown in Fig. 7-1. In this case, all nodal points on the boundary - except those at the free surface - and some points in the fluid domain are used to approximate the particular integrals. Figures 7-2 through 7-6 show the rate of conversions using various interior points. These figures show that the interior point is not required when Ω (= $\omega H/c$) is less than 3.0, but few interior points are required when Ω equals to 6.0. Comparison of the results obtained by using the proposed method against those obtained by the finite element method, for the element mesh shown in Fig. 7-7, is shown in Figs. 7-8 through 7-10. The results obtained are almost the same, except for small differences in the imaginary part of the hydrodynamic pressure when Ω equals to 6.0. The proposed method yields good accuracy!

Example 2: Response of the Coupled System of a Concrete Gravity Dam and Reservoir

Figure 7-11 shows a dam with two slopes on the upstream surface, and a reservoir which extends to infinity in the upstream direction. In this example, the floor of the reservoir and the foundation of the dam are assumed to be rigid. The finite element method, the boundary element method with particular integrals, and the modal analysis technique will be used to obtain a solution. Figure 7-12 shows the finite element mesh of the dam structure, and the boundary element mesh of the near field of the fluid domain. The finite element mesh in the dam structure consists of 144 quadrilateral plane stress elements, 171 nodal points and constraints at the base, for a total of 324 degrees-of-freedom. The boundary element mesh for the near field of the fluid domain includes 39 nodal points, 19 quadratic elements and 16 interior points (for the purpose of safety). The particular numerical values that are used in this example are:

Elastic Modulus $E = 3.5 \times 10^{6} T/m^{2}$
Poisson's Ratio $\nu = 0.2$
Weight Density of Concrete = $2.45 T/m^{3}$
Damping Ratio $\zeta = 0.05$ of critical in all vibration modes
Sound Velocity in Water C = 1438.656m/sec

The computed natural frequencies of the first six modes of the dam without water are 4.069, 9.249, 10.95, 16.57, 23.67 and 24.63 Hz, respectively. Their corresponding mode shapes are

shown in Figs. 7-13 through 7-18. The comparison of the complex responses of the dam without water, and with a full reservoir (including and excluding compressibility of water) is shown in Fig. 7-19. From the numerical results, it is seen that interactions of the dam containing water has the effect of reducing the natural frequencies of vibration of the dam. For the case where the compressibility of the water is included, the response is highly resonant at/and near the fundamental frequency of the combined system. However, the response is significantly reduced at the higher excitation frequencies, when compared to the case where water compressibility is neglected. This is because the effect of radiation damping associated with water compressibility is added to the effect of structural damping present in the dam. The peak responses of the system at the second and higher natural frequencies are quite small.

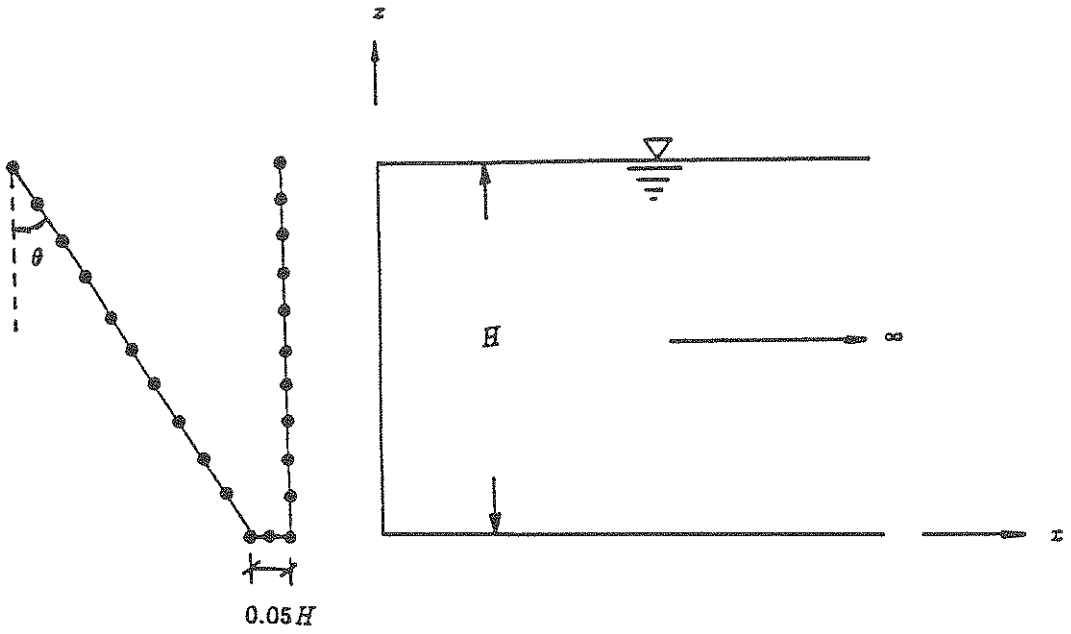

FIGURE 7-1 Boundary Element Mesh of the Dam with Sloping Angle, $\theta = 10^{\circ}$

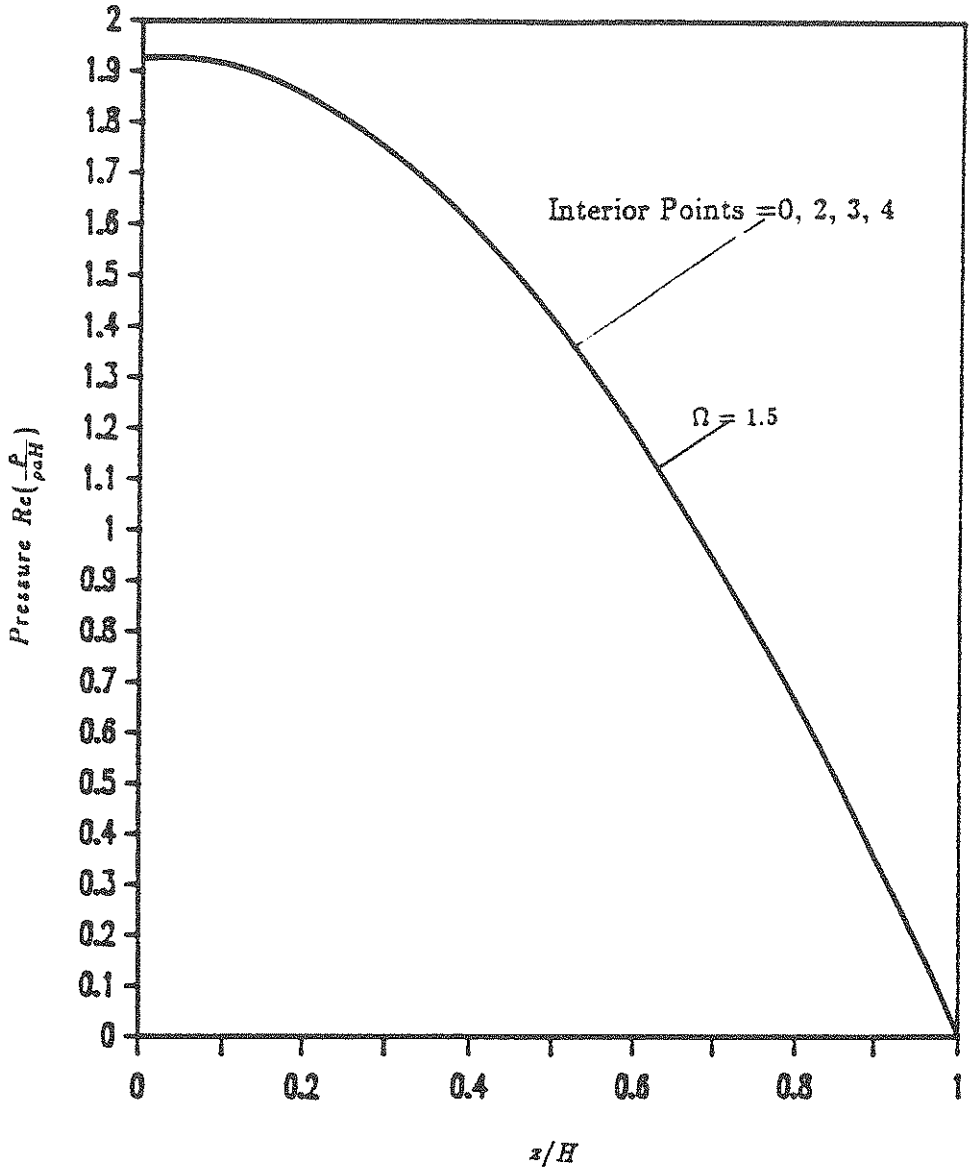

FIGURE 7-2 Hydrodynamic Pressures (Real Parts) Acting on the Dam with Sloping Angle $\theta = 10^{\circ}$ and with Frequency $\Omega = 1.5$. Results Are Almost Identical for Different Number of Interior Points

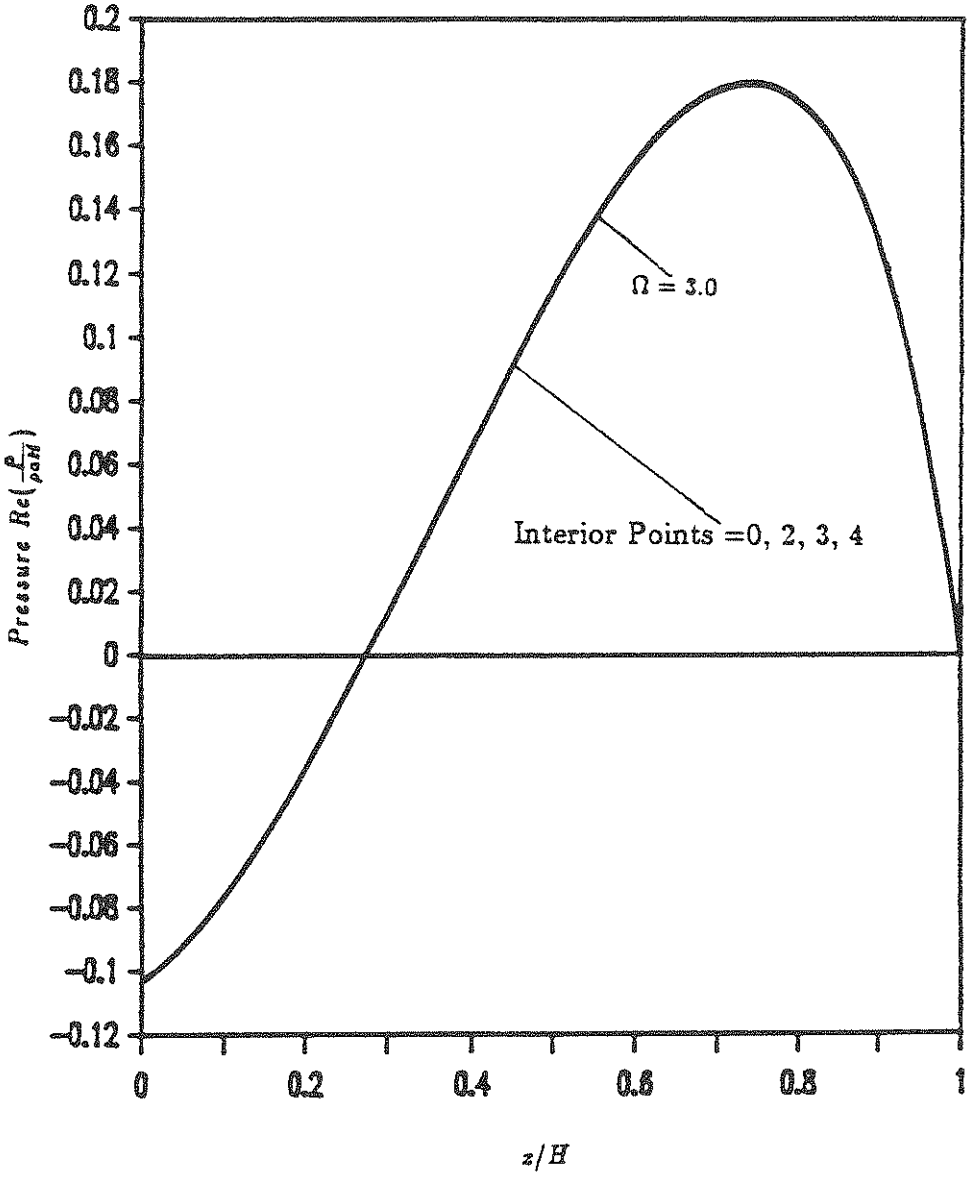

FIGURE 7-3 Hydrodynamic Pressures (Real Parts) Acting on the Dam with Sloping Angle, $\theta = 10^{\circ}$ and with Frequency $\Omega = 3.0$. Results Are Almost Identical for Different Number of Interior Points

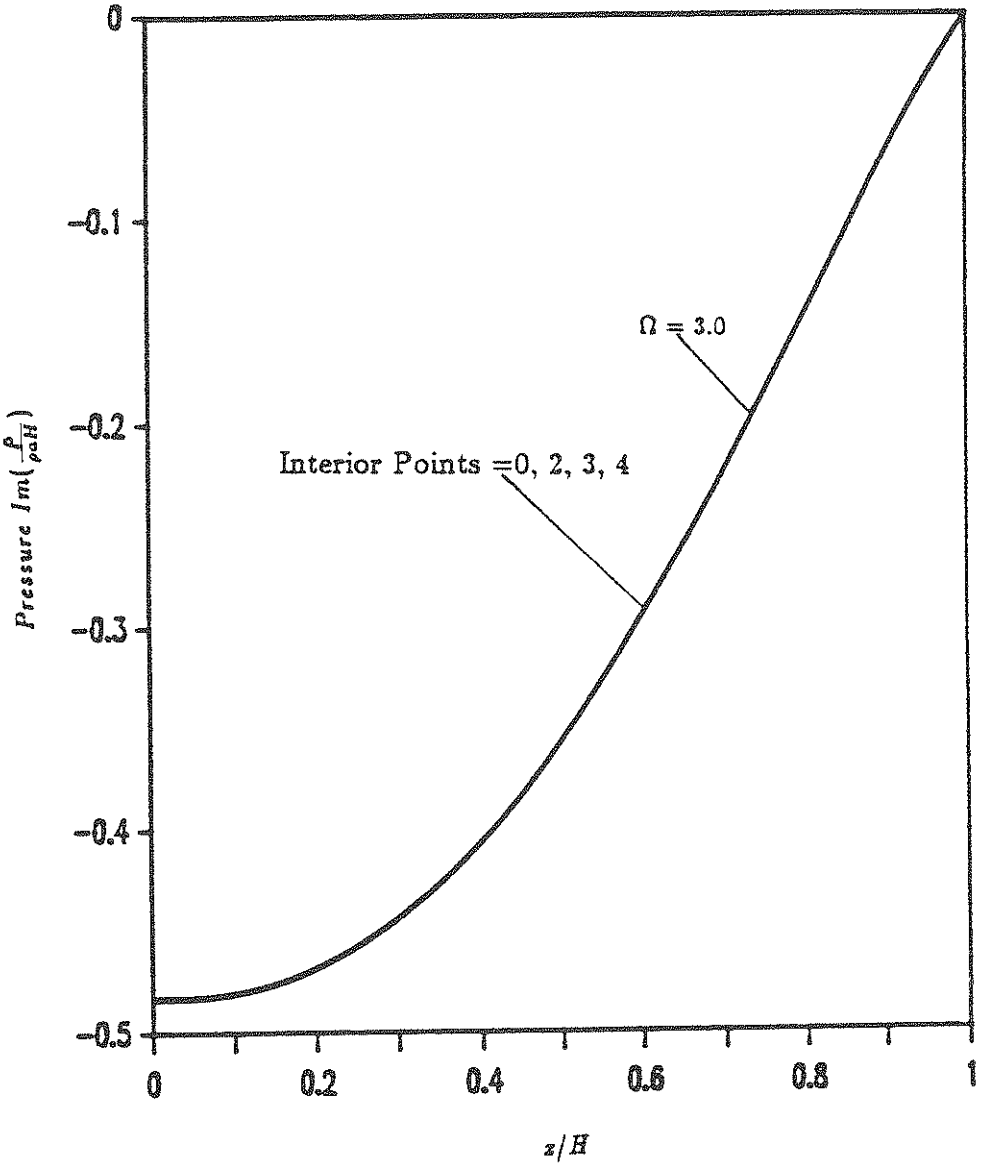

FIGURE 7-4 Hydrodynamic Pressures (Imaginary Parts) Acting on the Dam with Sloping Angle $\theta = 10^{\circ}$ and with Frequency $\Omega = 3.0$. Results Are Almost Identical for Different Number of Interior Points

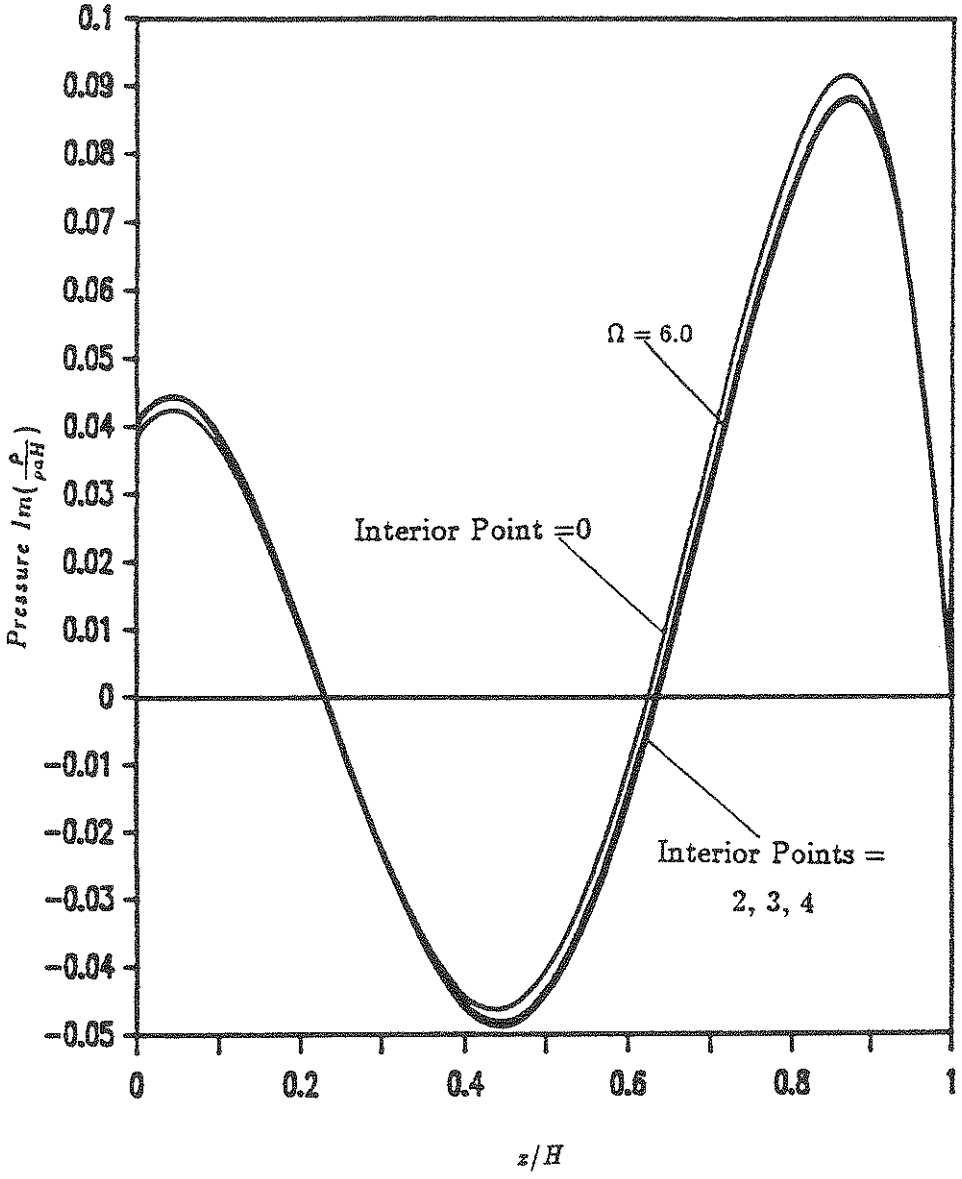

FIGURE 7-5 Hydrodynamic Pressures (Real Parts) Acting on the Dam with Sloping Angle, $\theta = 10^{\circ}$, and with Frequency $\Omega = 6.0$

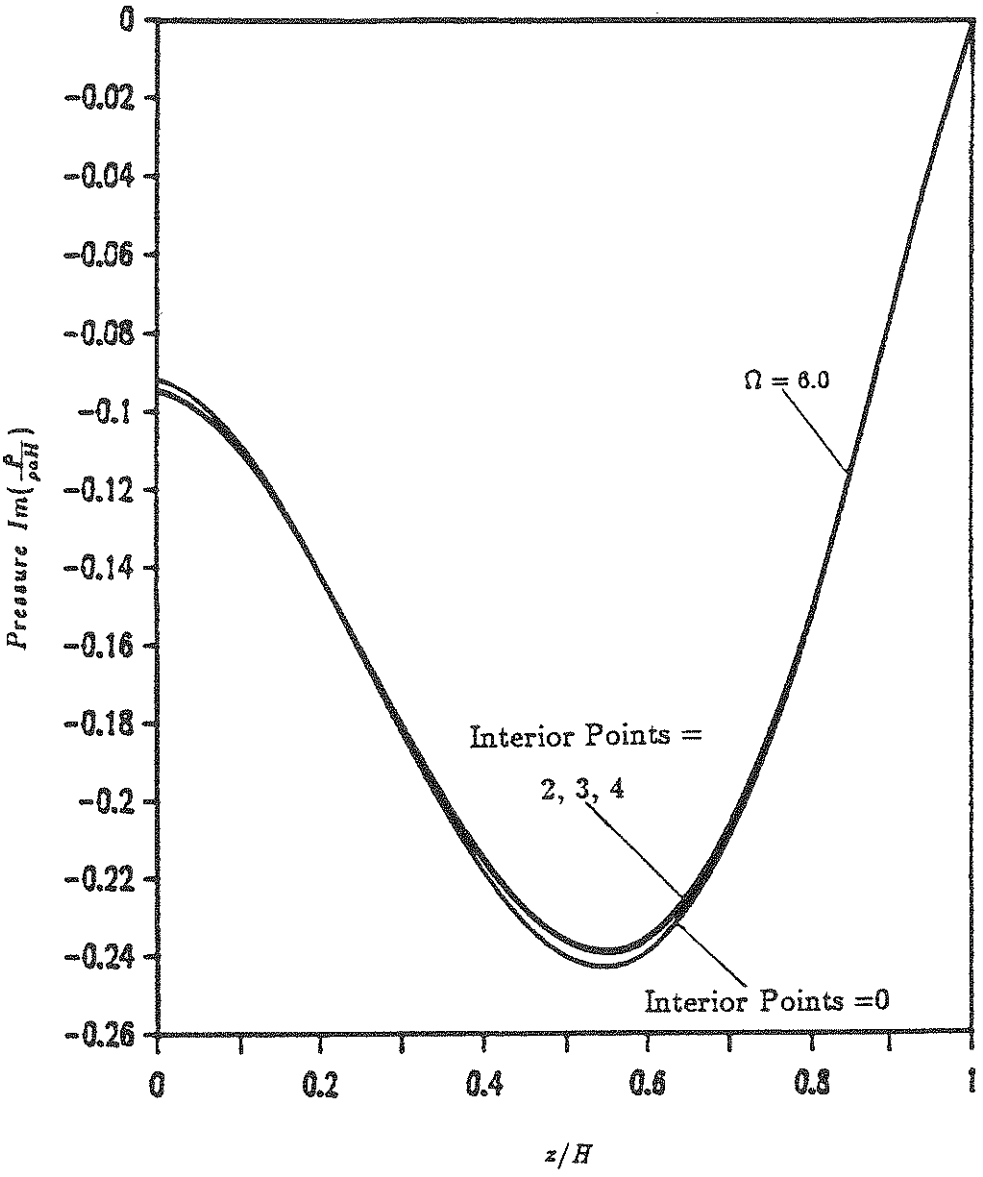

FIGURE 7-6 Hydrodynamic Pressures (Imaginary Parts) Acting on the Dam with Sloping Angle, $\theta = 10^{\circ}$, and with Frequency $\Omega = 6.0$

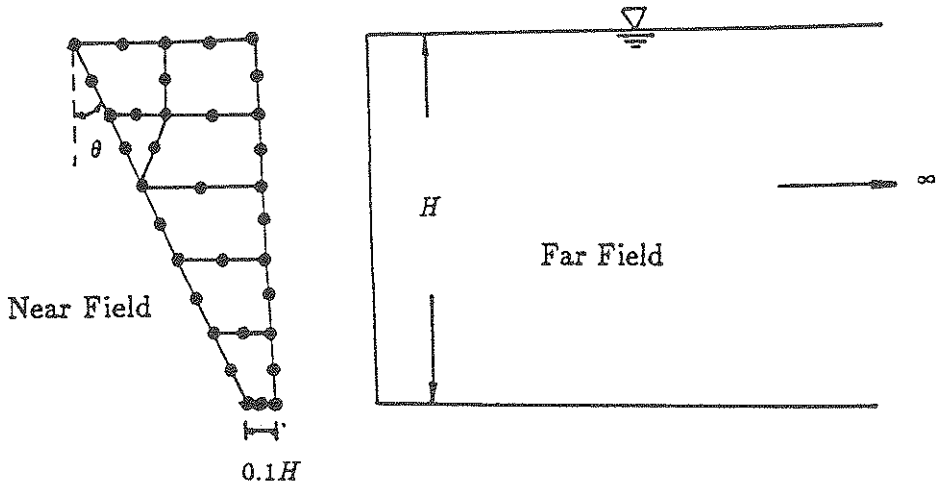

FIGURE 7-7 Finite Element Mesh of the Reservoir for the Dam with Sloping Angle $\theta = 10^{\circ}$

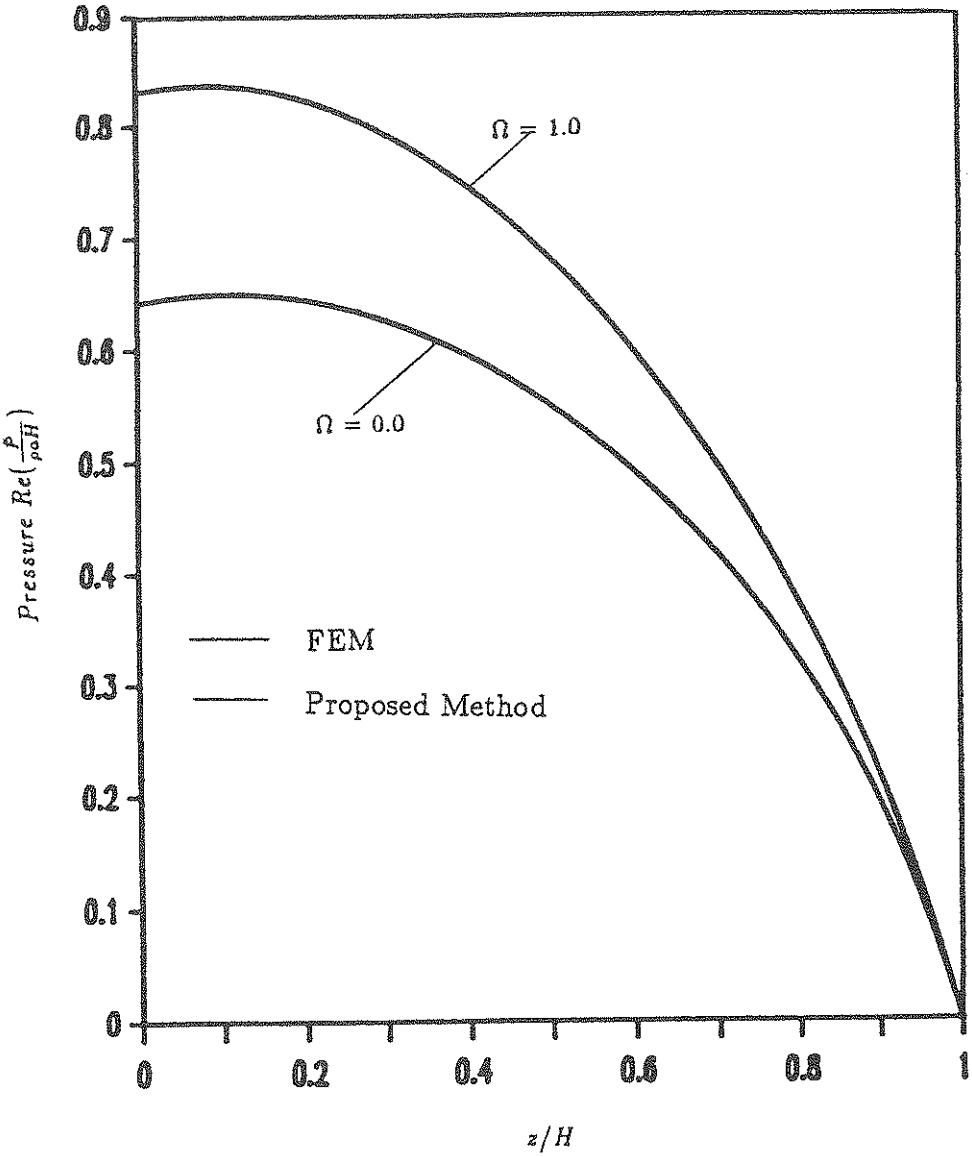

FIGURE 7-8 Hydrodynamic Pressures (Real Parts) Acting on the Dam with Sloping Angle, $\theta = 10^{\circ}$: Comparison of Results Between the Proposed Method and the Finite Element Method

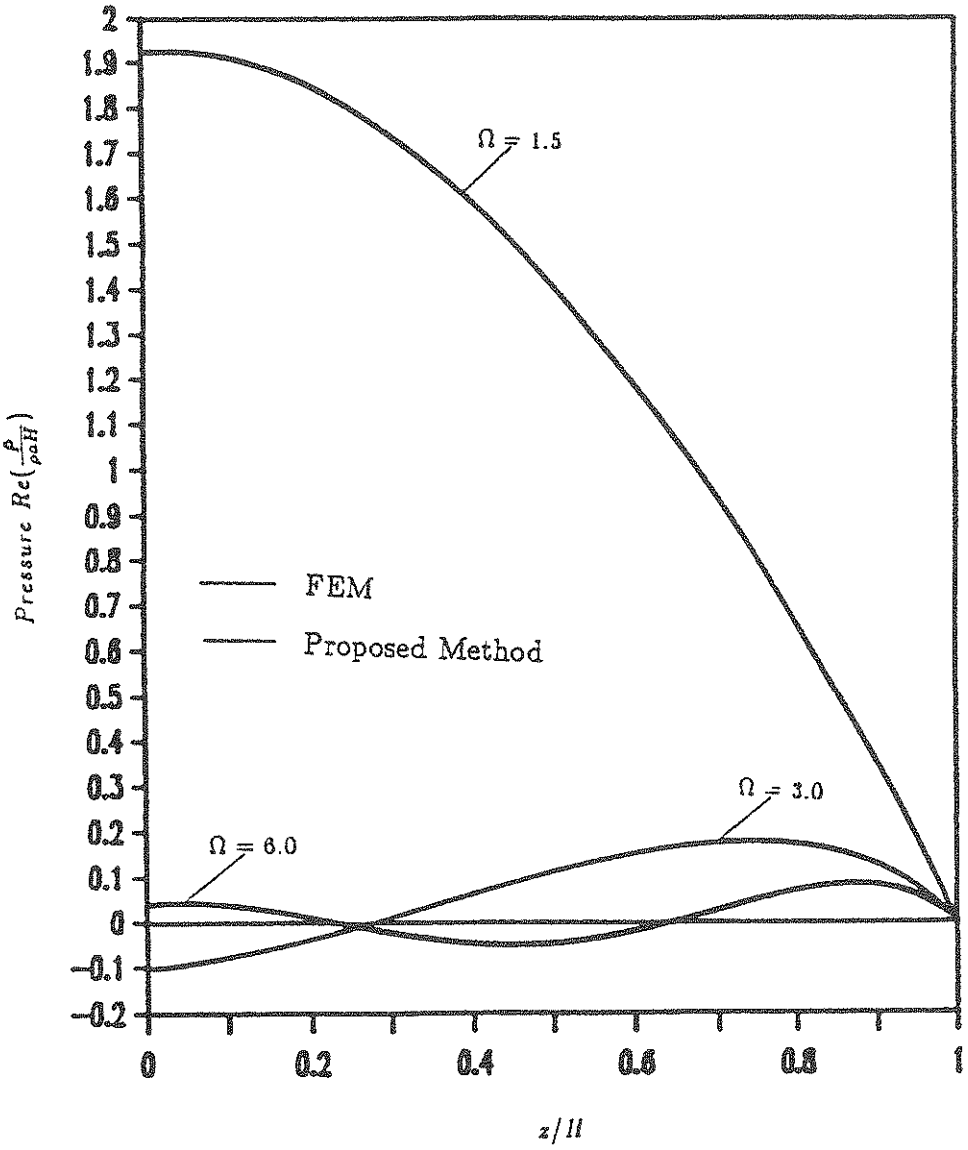

FIGURE 7-9 Hydrodynamic Pressures (Real Parts) Acting on the Dam with Sloping Angle, $\theta = 10^{\circ}$: Comparison of Results Between the Proposed Method and the Finite Element Method

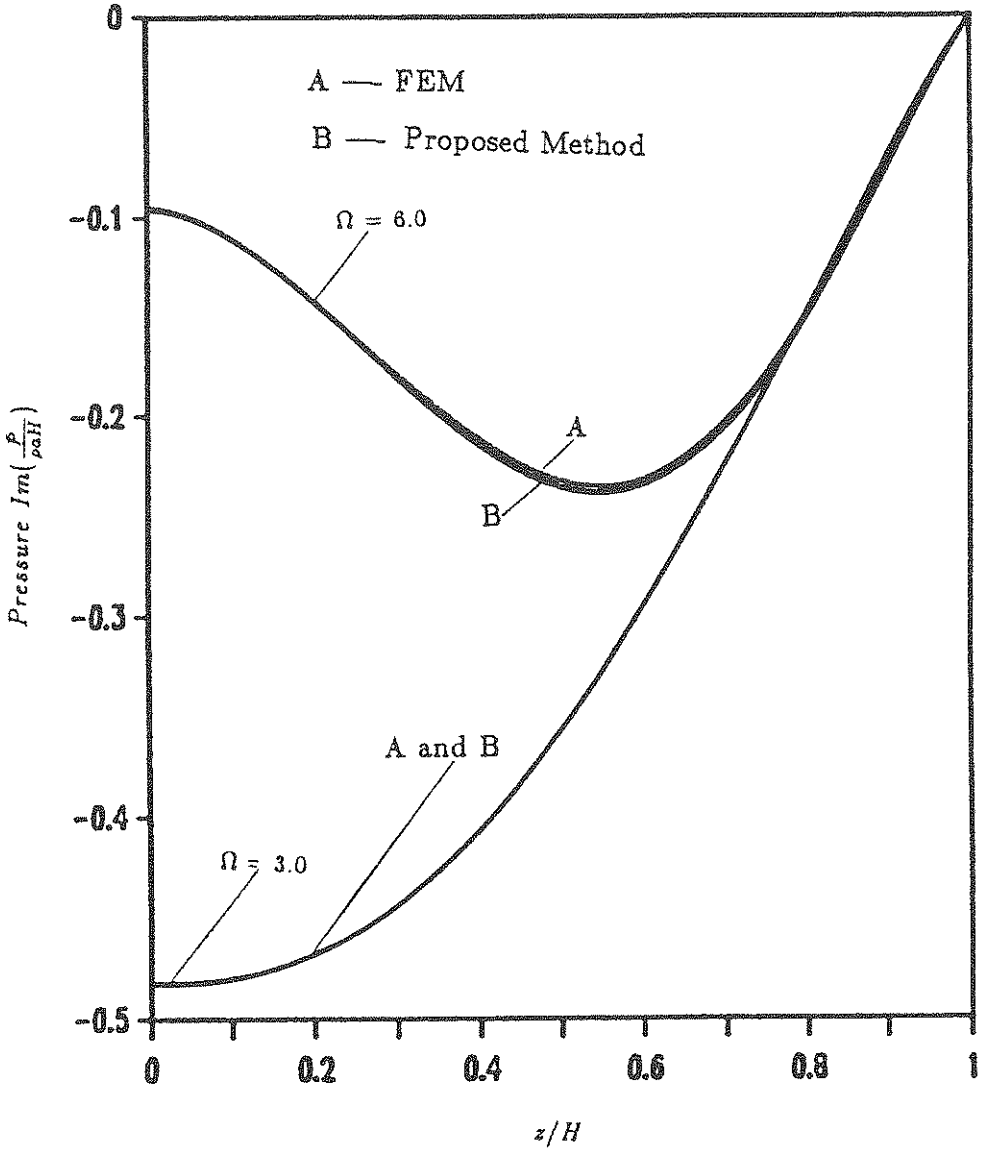

FIGURE 7-10 Hydrodynamic Pressures (Imaginary Parts) Acting on the Dam with Sloping Angle, $\theta = 10^{\circ}$: Comparison of Results Between the Proposed Method and the Finite Element Method

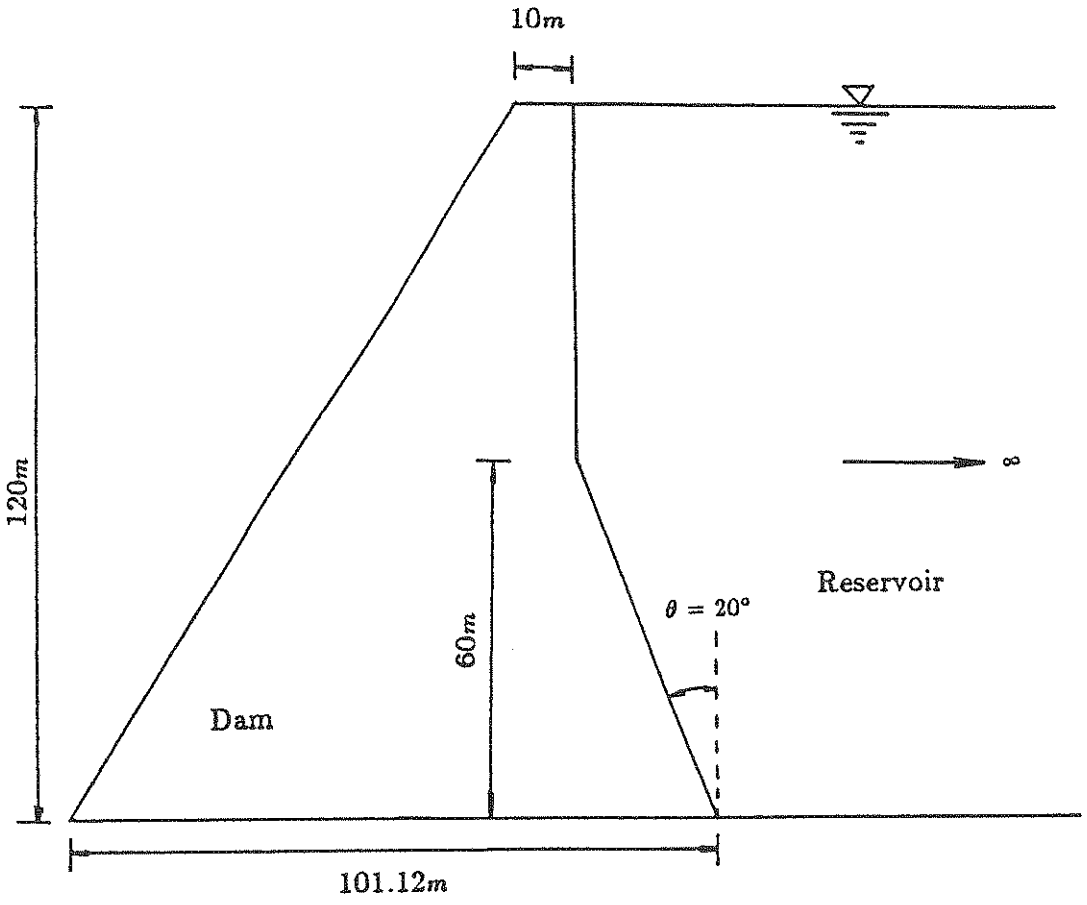

FIGURE 7-11 The Dam-Reservoir System of Example 2

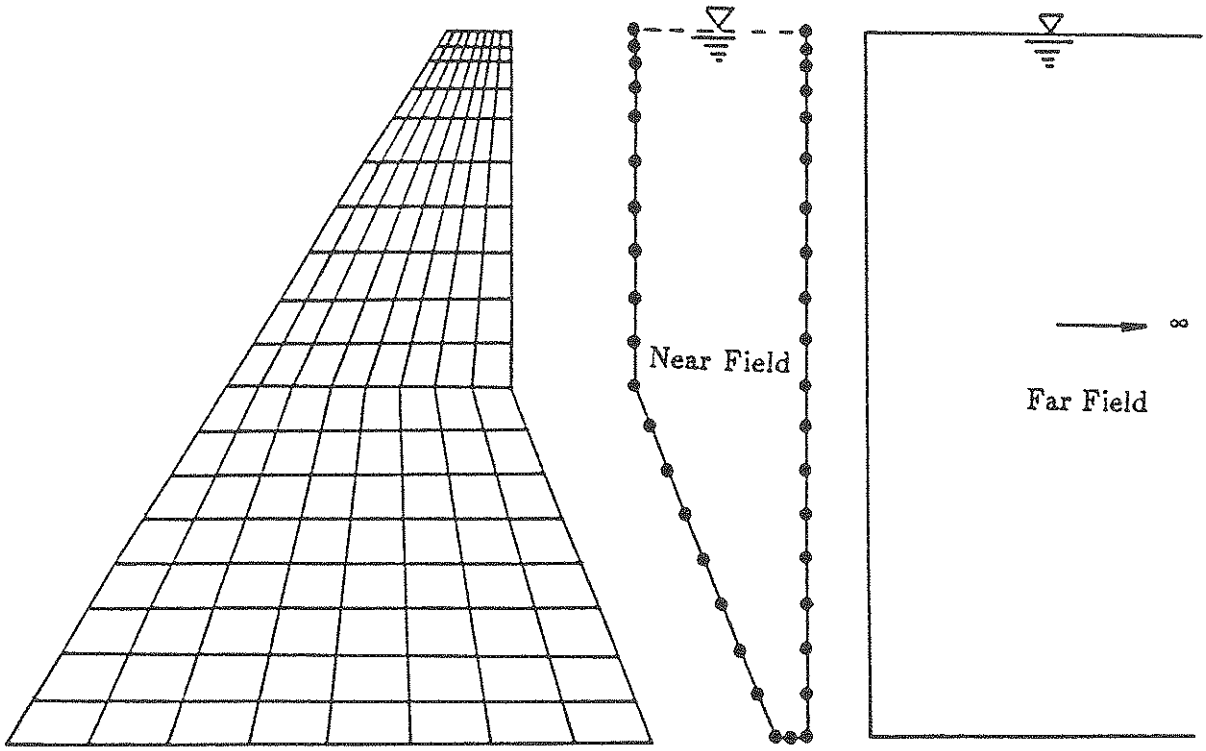

FIGURE 7-12 The Finite Element Mesh of the Dam Structure and the Boundary Element Mesh of the Near Field of the Fluid Domain in Example 2

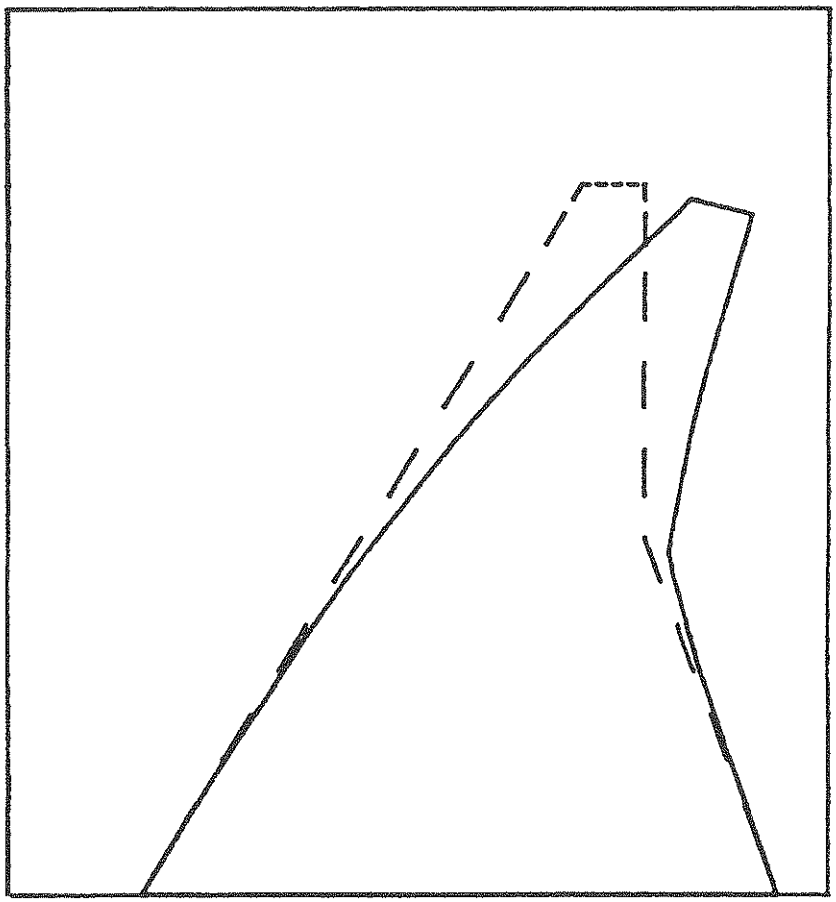

FIGURE 7-13 The First Mode Shape of the Dam Without Water in Example 2
Natural Frequency = 4.069 Hz

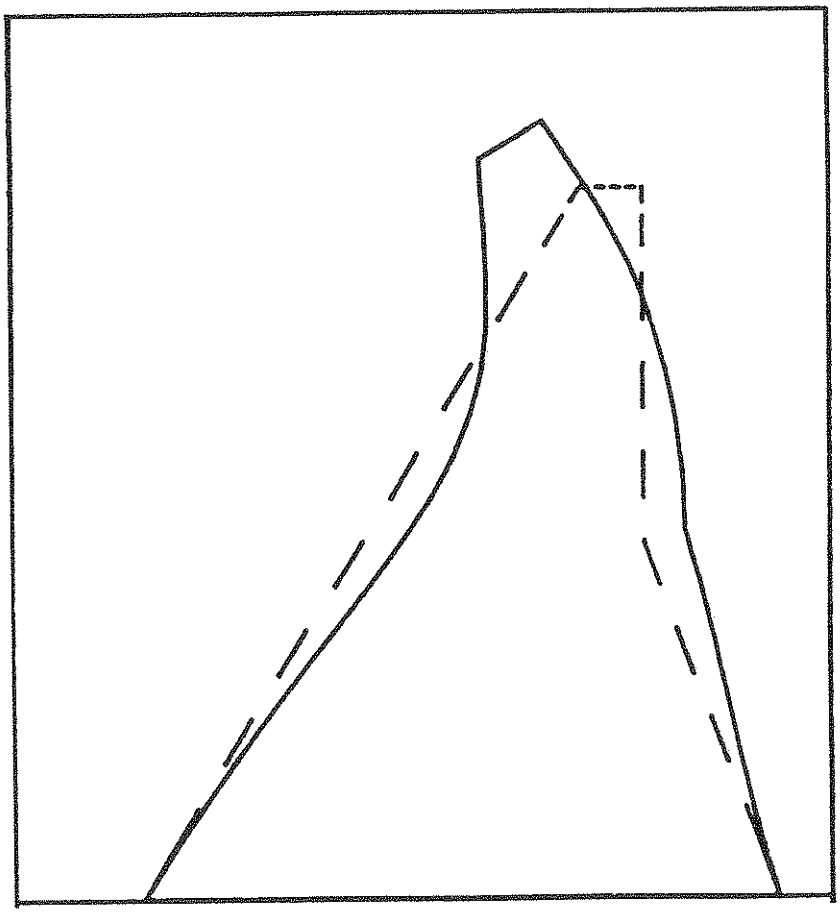

FIGURE 7-14 The Second Mode Shape of the Dam Without Water in Example 2
Natural Frequency = 9.249 Hz

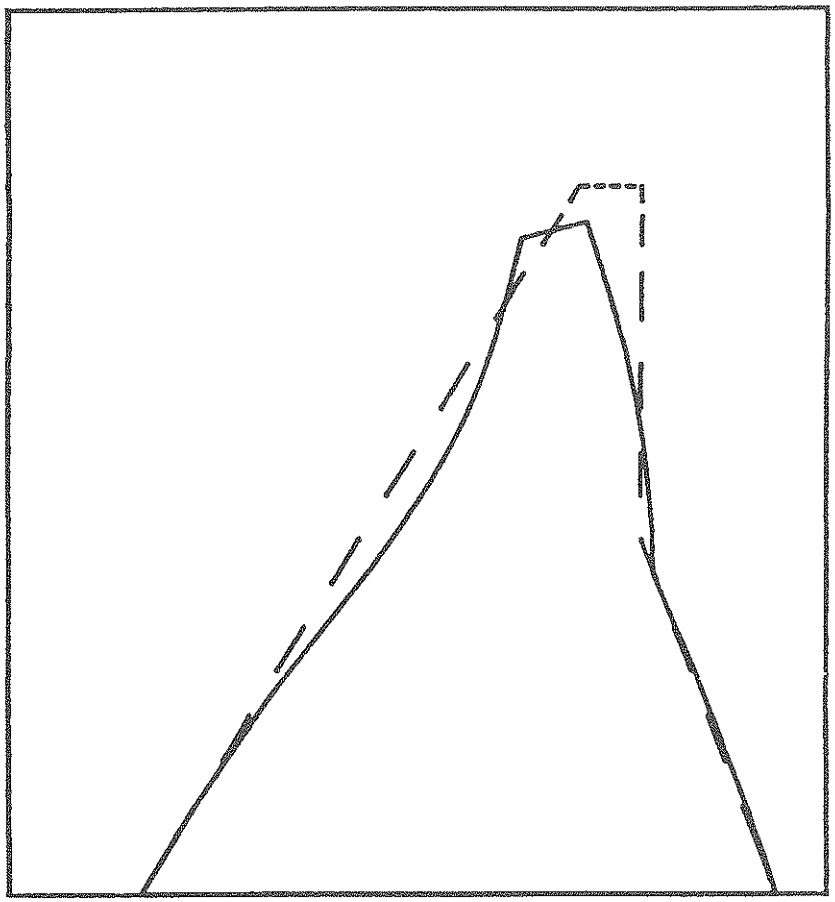

FIGURE 7-15 The Third Mode Shape of the Dam Without Water in Example 2
Natural Frequency = 10.95 Hz

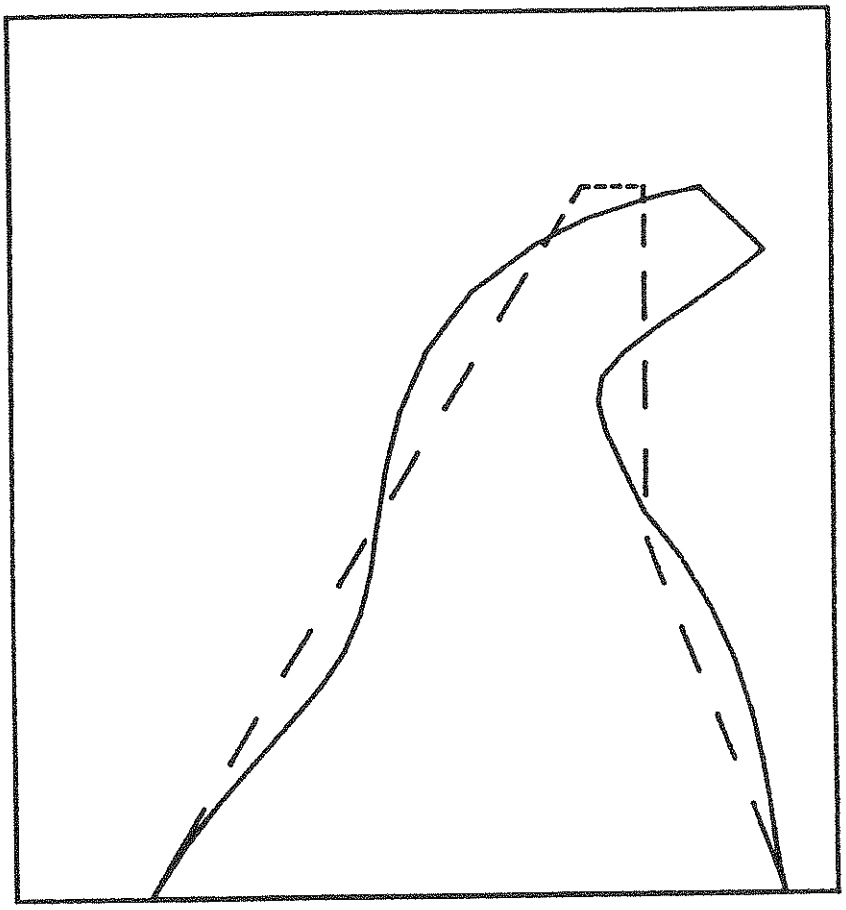

FIGURE 7-16 The Fourth Mode Shape of the Dam Without Water in Example 2
Natural Frequency = 16.57 Hz

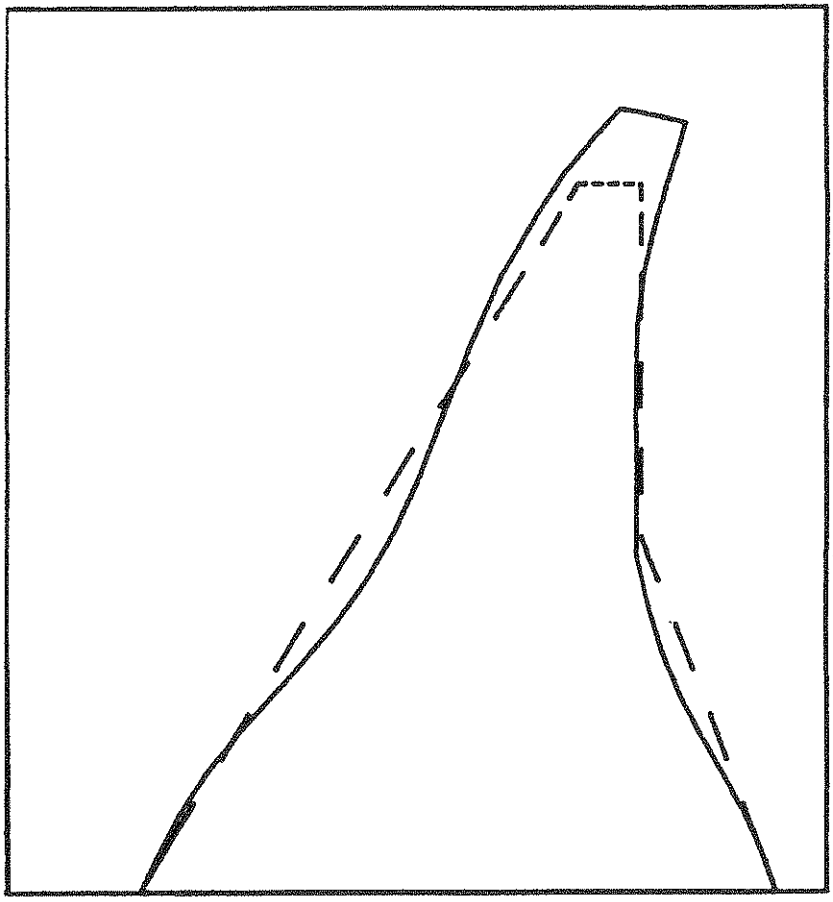

FIGURE 7-17 The Fifth Mode Shape of the Dam Without Water in Example 2
Natural Frequency = 23.67 Hz

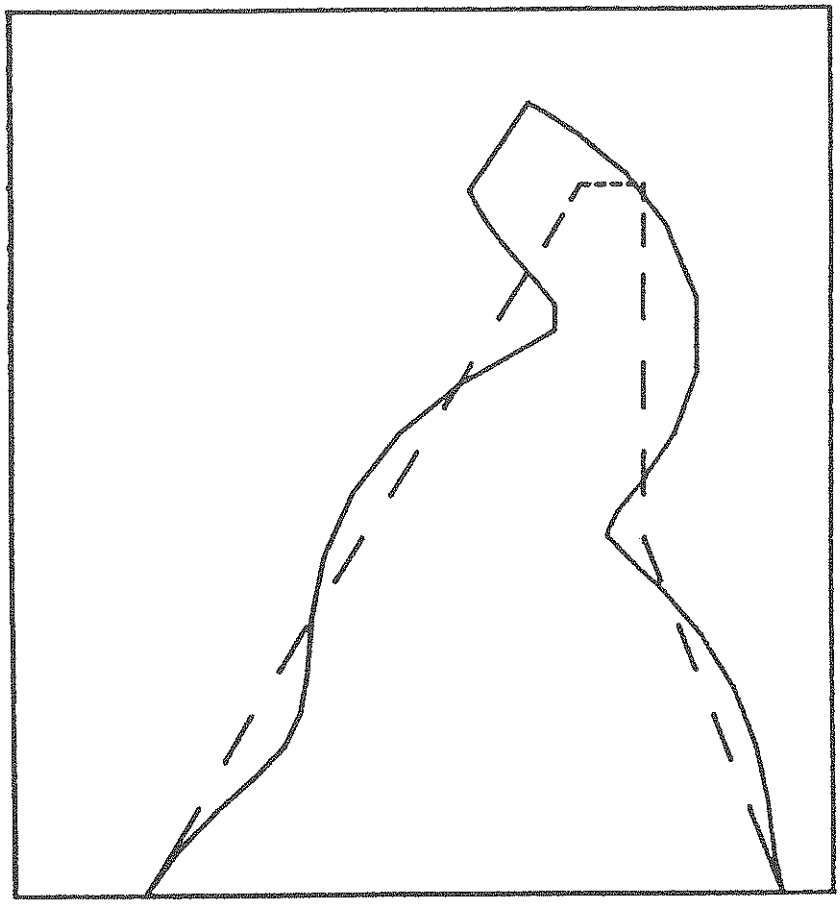

FIGURE 7-18 The Sixth Mode Shape of the Dam Without Water in Example 2
Natural Frequency = 24.63 Hz

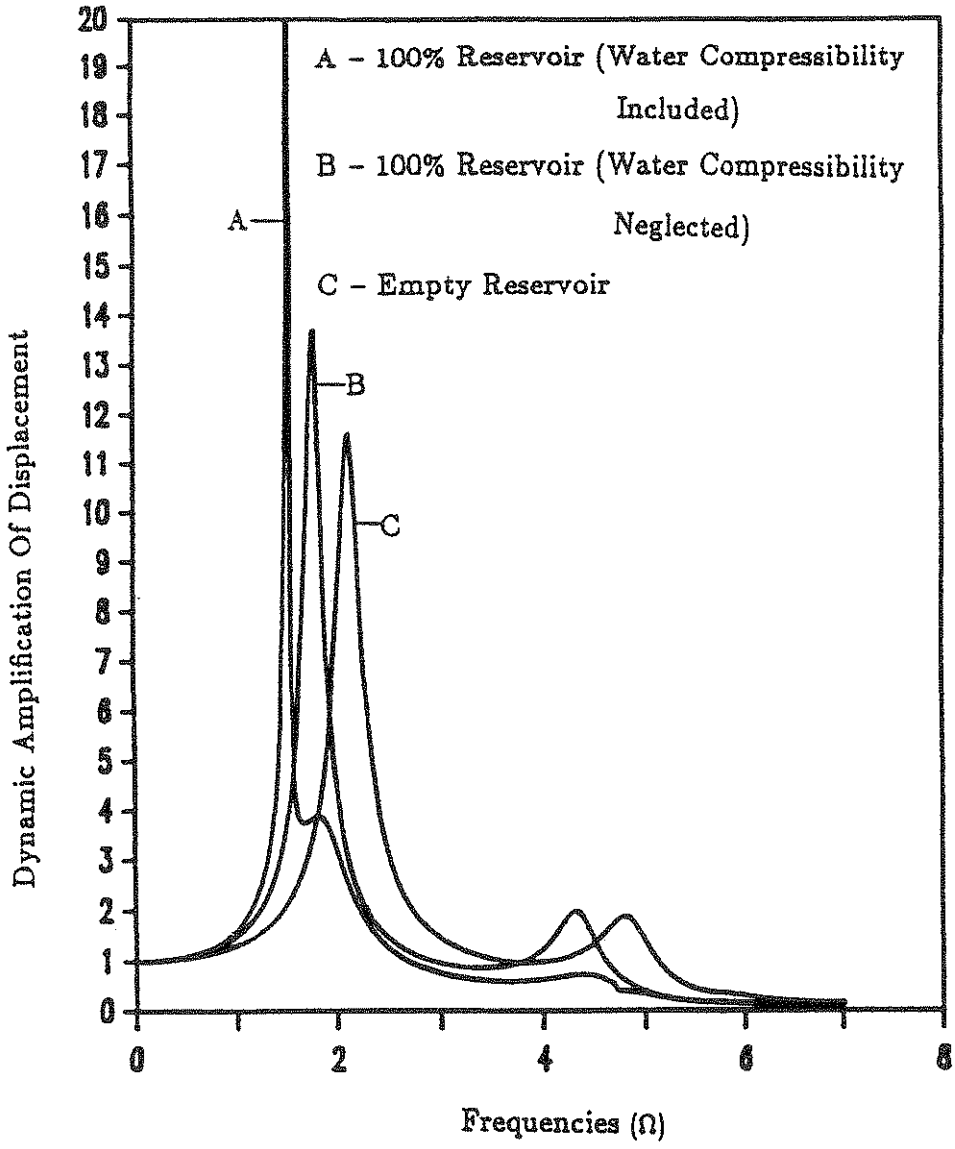

FIGURE 7-19 Frequency Response of the Dam of Example 2 Due to Horizontal Ground Motion

SECTION 8
CONCLUSIONS

The method described in this report, which allows frequency-independent fundamental solutions to be used to solve the scalar wave equation, and the boundary element method to be used in combination with another method, reduces the nonsymmetrical matrix to a very small size. Moreover, it is easier to understand the whole system behavior from the proposed formulations. When the reservoir is finite in size, the hydrodynamic response is real valued. For an infinite reservoir, it is complex. This important phenomena is clearly represented in the mathematical derivations.

Water compressibility has a significant effect on the response of the dam-reservoir system. Hydrodynamic effects reduce the natural frequencies.

SECTION 9
REFERENCES

1. Westergaard, H.M., "Water Pressures on Dams During Earthquakes," Transactions, ASCE, Vol. 98, 1933, pp. 418-433.

2. Zangar, C.N. and Haefeli, R.J., "Electric Analog Indicates Effect of Horizontal Earthquake Shock on Dams," Civil Engineering, April 1952, pp. 54-55, (Vol. pp. 278-279).

3. Zienkiewcz, O.C. and Nath Bhaskar, "Earthquake Hydrodynamic Pressures on Arch Dams - An Electric Analogue Solution," Proc. Inst. Civil Engineering, 25, 1963, pp. 165-176.

4. Chopra, A.K., "Hydrodynamic Pressures on Dams During Earthquakes," Journal of the Engineering Mechanics Division, Proc. of the ASCE, Vol. 93, No EM6, Dec. 1967, pp. 205-223.

5. Hanna, Y.G. and Humar, J.L., "Boundary Element Analysis of Fluid Domain," Journal of the Engineering Mechanics Division, Proc. of the ASCE, Vol. 108, No. EM2, April 1982, pp. 436-450.

6. Chopra, A.K., "Earthquake Response of Concrete Gravity Dams," Journal of the Engineering Mechanics Division, Proc. of the ASCE, Vol. 96, No. EM4, Aug. 1970, pp. 443-454.

7. Chakrabarti, P. and Chopra, A.K., "Earthquake Analysis of Gravity Dams Including Hydrodynamic Interaction," Earthquake Engineering and Structural Dynamics, Vol. 2, 1973, pp. 143-160.

8. Liaw, C-Y. and Chopra, A.K., "Dynamics of Towers Surrounded by Water," Earthquake Engineering and Structural Dynamics, Vol 3, 1974, pp. 33-49.

9. Saini, S.S., Bettess, P. and Zienkiewicz, O.C., "Coupled Hydrodynamic Response of Concrete Gravity Dams Using Finite and Infinite Elements," Earthquake Engineering and Structural Dynamics, Vol. 6, 1978, pp. 363-374.

10. Hall, J.F. and Chopra, A.K., "Dynamic Response of Embankment, Concrete-Gravity and Arch Dams Including Hydrodynamic Interaction," Earthquake Engineering Research Center, Report No. EERC 80-39, U.C. Berkeley, California, Oct. 1980.

11. Porter, Craig S. and Chopra, A.K., "Hydrodynamic Effects in Dynamic Response of Simple Arch Dams," Earthquake Engineering and Structural Dynamics, Vol. 10, 1982, pp. 417-431.

12. Kuo, J.S-H., "Fluid-Structure Interactions: Added-Mass Computations for Incompressible Fluid," Earthquake Engineering Research Center, Report No. EERC 82-09, U.C. Berkeley, California, Aug. 1982.

13. Clough, R.W., Stephen, R.M. and Kuo, J.S-H., "Dynamic Response Analysis of Techi Dam," Earthquake Engineering Research Center, Report No. EERC 82-11, U.C. Berkeley, California, Aug. 1982.

14. Tsai, C.S. and Lee, George C., "Arch Dam-Fluid Interactions: by FEM-BEM and Substructure Concept," International Journal for Numberical Methods in Engineering, Vol. 24, Dec. 1987, pp. 2367-2388.

15. Tsai, C.S. and Lee, George C., "Analyses of Infinite Reservoir Using the Boundary Element Method With Particular Integrals," Boundary Elements IX, Proceedings of the 9th International Conference, West Germany, September 1987, Vol. 1, pp. 143-164.

16. Tsai, C.S. and Lee, George C., "Analyses of Infinite Reservoir," ASCE Engineering Mechanics Specialty Conference, State University of New York at Buffalo, May 1987.

17. Tsai, C.S. and Lee, George C., "Hydrodynamic Pressure on Gravity Dams Subjected to Ground Motion," Accepted by the Engineering Mechanics Division, Proc. of the ASCE.

18. Ohta, K., Kagawa, K. and Honda, I., "Analysis of Fluid-Structure Vibration Using Boundary Element Method and Modal Analysis Technique," Proceedings of the 1985 Pressure Vessels and Piping Conference, Fluid-Structure Dynamics, PVP Vol. 98-7, pp. 215-220.

19. Clough, R.W. and Penzien, J., "Dynamics of Structures," McGraw-Hill, 1975.

20. Thomson, W.T., "Theory of Vibration with Application," Prentice-Hall, Inc., 1972.

NATIONAL CENTER FOR EARTHQUAKE ENGINEERING RESEARCH
LIST OF PUBLISHED TECHNICAL REPORTS

The National Center for Earthquake Engineering Research (NCEER) publishes technical reports on a variety of subjects related to earthquake engineering written by authors funded through NCEER. These reports are available from both NCEER's Publications Department and the National Technical Information Service (NTIS). Requests for reports should be directed to the Publications Department, National Center for Earthquake Engineering Research, State University of New York at Buffalo, Red Jacket Quadrangle, Buffalo, New York 14261. Reports can also be requested through NTIS, 5285 Port Royal Road, Springfield, Virginia 22161. NTIS accession numbers are shown in parenthesis, if available.

NCEER-87-0001 "First-Year Program in Research, Education and Technology Transfer," 3/5/87, (PB88-134275/AS).

NCEER-87-0002 "Experimental Evaluation of Instantaneous Optimal Algorithms for Structural Control," by R.C. Lin, T.T. Soong and A.M. Reinhorn, 4/20/87, (PB88-134341/AS).

NCEER-87-0003 "Experimentation Using the Earthquake Simulation Facilities at University at Buffalo," by A.M. Reinhorn and R.L. Ketter, to be published.

NCEER-87-0004 "The System Characteristics and Performance of a Shaking Table," by J.S. Hwang, K.C. Chang and G.C. Lee, 6/1/87, (PB88-134259/AS).

NCEER-87-0005 "A Finite Element Formulation for Nonlinear Viscoplastic Material Using a Q Model," by O. Gyebi and G. Dasgupta, 11/2/87, (PB88-213764/AS).

NCEER-87-0006 "Symbolic Manipulation Program (SMP) - Algebraic Codes for Two and Three Dimensional Finite Element Formulations," by X. Lee and G. Dasgupta, 11/9/87, (PB88-219522/AS).

NCEER-87-0007 "Instantaneous Optimal Control Laws for Tall Buildings Under Seismic Excitations," by J.N. Yang, A. Akbarpour and P. Ghaemmaghami, 6/10/87, (PB88-134333/AS).

NCEER-87-0008 "IDARC: Inelastic Damage Analysis of Reinforced Concrete Frame - Shear-Wall Structures," by Y.J. Park, A.M. Reinhorn and S.K. Kunnath, 7/20/87, (PB88-134325/AS).

NCEER-87-0009 "Liquefaction Potential for New York State: A Preliminary Report on Sites in Manhattan and Buffalo," by M. Budhu, V. Vijayakumar, R.F. Giese and L. Baumgras, 8/31/87, (PB88-163704/AS). This report is available only through NTIS (see address given above).

NCEER-87-0010 "Vertical and Torsional Vibration of Foundations in Inhomogeneous Media," by A.S. Veletsos and K.W. Dotson, 6/1/87, (PB88-134291/AS).

NCEER-87-0011 "Seismic Probabilistic Risk Assessment and Seismic Margins Studies for Nuclear Power Plants," by Howard H.M. Hwang, 6/15/87, (PB88-134267/AS). This report is available only through NTIS (see address given above).

NCEER-87-0012 "Parametric Studies of Frequency Response of Secondary Systems Under Ground-Acceleration Excitations," by Y. Yong and Y.K. Lin, 6/10/87, (PB88-134309/AS).

NCEER-87-0013 "Frequency Response of Secondary Systems Under Seismic Excitation," by J.A. HoLung, J. Cai and Y.K. Lin, 7/31/87, (PB88-134317/AS).

NCEER-87-0014 "Modelling Earthquake Ground Motions in Seismically Active Regions Using Parametric Time Series Methods," by G.W. Ellis and A.S. Cakmak, 8/25/87, (PB88-134283/AS).

NCEER-87-0015 "Detection and Assessment of Seismic Structural Damage," by E. DiPasquale and A.S. Cakmak, 8/25/87, (PB88-163712/AS).

NCEER-87-0016 "Pipeline Experiment at Parkfield, California," by J. Isenberg and E. Richardson, 9/15/87, (PB88-163720/AS).

NCEER-87-0017 "Digital Simulation of Seismic Ground Motion," by M. Shinozuka, G. Deodatis and T. Harada, 8/31/87, (PB88-155197/AS). This report is available only through NTIS (see address given above).

NCEER-87-0018 "Practical Considerations for Structural Control: System Uncertainty, System Time Delay and Truncation of Small Control Forces," J.N. Yang and A. Akbarpour, 8/10/87, (PB88-163738/AS).

NCEER-87-0019 "Modal Analysis of Nonclassically Damped Structural Systems Using Canonical Transformation," by J.N. Yang, S. Sarkani and F.X. Long, 9/27/87, (PB88-187851/AS).

NCEER-87-0020 "A Nonstationary Solution in Random Vibration Theory," by J.R. Red-Horse and P.D. Spanos, 11/3/87, (PB88-163746/AS).

NCEER-87-0021 "Horizontal Impedances for Radially Inhomogeneous Viscoelastic Soil Layers," by A.S. Veletsos and K.W. Dotson, 10/15/87, (PB88-150859/AS).

NCEER-87-0022 "Seismic Damage Assessment of Reinforced Concrete Members," by Y.S. Chung, C. Meyer and M. Shinozuka, 10/9/87, (PB88-150867/AS). This report is available only through NTIS (see address given above).

NCEER-87-0023 "Active Structural Control in Civil Engineering," by T.T. Soong, 11/11/87, (PB88-187778/AS).

NCEER-87-0024 Vertical and Torsional Impedances for Radially Inhomogeneous Viscoelastic Soil Layers," by K.W. Dotson and A.S. Veletsos, 12/87, (PB88-187786/AS).

NCEER-87-0025 "Proceedings from the Symposium on Seismic Hazards, Ground Motions, Soil-Liquefaction and Engineering Practice in Eastern North America," October 20-22, 1987, edited by K.H. Jacob, 12/87, (PB88-188115/AS).

NCEER-87-0026 "Report on the Whittier-Narrows, California, Earthquake of October 1, 1987," by J. Pantelic and A. Reinhorn, 11/87, (PB88-187752/AS). This report is available only through NTIS (see address given above).

NCEER-87-0027 "Design of a Modular Program for Transient Nonlinear Analysis of Large 3-D Building Structures," by S. Srivastav and J.F. Abel, 12/30/87, (PB88-187950/AS).

NCEER-87-0028 "Second-Year Program in Research, Education and Technology Transfer," 3/8/88, (PB88-219480/AS).

NCEER-88-0001 "Workshop on Seismic Computer Analysis and Design of Buildings With Interactive Graphics," by W. McGuire, J.F. Abel and C.H. Conley, 1/18/88, (PB88-187760/AS).

NCEER-88-0002 "Optimal Control of Nonlinear Flexible Structures," by J.N. Yang, F.X. Long and D. Wong, 1/22/88, (PB88-213772/AS).

NCEER-88-0003 "Substructuring Techniques in the Time Domain for Primary-Secondary Structural Systems," by G.D. Manolis and G. Juhn, 2/10/88, (PB88-213780/AS).

NCEER-88-0004 "Iterative Seismic Analysis of Primary-Secondary Systems," by A. Singhal, L.D. Lutes and P.D. Spanos, 2/23/88, (PB88-213798/AS).

NCEER-88-0005 "Stochastic Finite Element Expansion for Random Media," by P.D. Spanos and R. Ghanem, 3/14/88, (PB88-213806/AS).

NCEER-88-0006 "Combining Structural Optimization and Structural Control," by F.Y. Cheng and C.P. Pantelides, 1/10/88, (PB88-213814/AS).

NCEER-88-0007 "Seismic Performance Assessment of Code-Designed Structures," by H.H-M. Hwang, J-W. Jaw and H-J. Shau, 3/20/88, (PB88-219423/AS).

NCEER-88-0008 "Reliability Analysis of Code-Designed Structures Under Natural Hazards," by H.H-M. Hwang, H. Ushiba and M. Shinozuka, 2/29/88, (PB88-229471/AS).

NCEER-88-0009 "Seismic Fragility Analysis of Shear Wall Structures," by J-W Jaw and H.H-M. Hwang, 4/30/88, (PB89-102867/AS).

NCEER-88-0010 "Base Isolation of a Multi-Story Building Under a Harmonic Ground Motion - A Comparison of Performances of Various Systems," by F-G Fan, G. Ahmadi and I.G. Tadjbakhsh, 5/18/88, (PB89-122238/AS).

NCEER-88-0011 "Seismic Floor Response Spectra for a Combined System by Green's Functions," by F.M. Lavelle, L.A. Bergman and P.D. Spanos, 5/1/88, (PB89-102875/AS).

NCEER-88-0012 "A New Solution Technique for Randomly Excited Hysteretic Structures," by G.Q. Cai and Y.K. Lin, 5/16/88, (PB89-102883/AS).

NCEER-88-0013 "A Study of Radiation Damping and Soil-Structure Interaction Effects in the Centrifuge," by K. Weissman, supervised by J.H. Prevost, 5/24/88, (PB89-144703/AS).

NCEER-88-0014 "Parameter Identification and Implementation of a Kinematic Plasticity Model for Frictional Soils," by J.H. Prevost and D.V. Griffiths, to be published.

NCEER-88-0015 "Two- and Three- Dimensional Dynamic Finite Element Analyses of the Long Valley Dam," by D.V. Griffiths and J.H. Prevost, 6/17/88, (PB89-144711/AS).

NCEER-88-0016 "Damage Assessment of Reinforced Concrete Structures in Eastern United States," by A.M. Reinhorn, M.J. Seidel, S.K. Kunnath and Y.J. Park, 6/15/88, (PB89-122220/AS).

NCEER-88-0017 "Dynamic Compliance of Vertically Loaded Strip Foundations in Multilayered Viscoelastic Soils," by S. Ahmad and A.S.M. Israil, 6/17/88, (PB89-102891/AS).

NCEER-88-0018 "An Experimental Study of Seismic Structural Response With Added Viscoelastic Dampers," by R.C. Lin, Z. Liang, T.T. Soong and R.H. Zhang, 6/30/88, (PB89-122212/AS).

NCEER-88-0019 "Experimental Investigation of Primary - Secondary System Interaction," by G.D. Manolis, G. Juhn and A.M. Reinhorn, 5/27/88, (PB89-122204/AS).

NCEER-88-0020 "A Response Spectrum Approach For Analysis of Nonclassically Damped Structures," by J.N. Yang, S. Sarkani and F.X. Long, 4/22/88, (PB89-102909/AS).

NCEER-88-0021 "Seismic Interaction of Structures and Soils: Stochastic Approach," by A.S. Veletsos and A.M. Prasad, 7/21/88, (PB89-122196/AS).

NCEER-88-0022 "Identification of the Serviceability Limit State and Detection of Seismic Structural Damage," by E. DiPasquale and A.S. Cakmak, 6/15/88, (PB89-122188/AS).

NCEER-88-0023 "Multi-Hazard Risk Analysis: Case of a Simple Offshore Structure," by B.K. Bhartia and E.H. Vanmarcke, 7/21/88, (PB89-145213/AS).

NCEER-88-0024 "Automated Seismic Design of Reinforced Concrete Buildings," by Y.S. Chung, C. Meyer and M. Shinozuka, 7/5/88, (PB89-122170/AS).

NCEER-88-0025 "Experimental Study of Active Control of MDOF Structures Under Seismic Excitations," by L.L. Chung, R.C. Lin, T.T. Soong and A.M. Reinhorn, 7/10/88, (PB89-122600/AS).

NCEER-88-0026 "Earthquake Simulation Tests of a Low-Rise Metal Structure," by J.S. Hwang, K.C. Chang, G.C. Lee and R.L. Ketter, 8/1/88, (PB89-102917/AS).

NCEER-88-0027 "Systems Study of Urban Response and Reconstruction Due to Catastrophic Earthquakes," by F. Kozin and H.K. Zhou, 9/22/88, to be published.

NCEER-88-0028 "Seismic Fragility Analysis of Plane Frame Structures," by H.H-M. Hwang and Y.K. Low, 7/31/88, (PB89-131445/AS).

NCEER-88-0029 "Response Analysis of Stochastic Structures," by A. Kardara, C. Bucher and M. Shinozuka, 9/22/88.

NCEER-88-0030 "Nonnormal Accelerations Due to Yielding in a Primary Structure," by D.C.K. Chen and L.D. Lutes, 9/19/88, (PB89-131437/AS).

NCEER-88-0031 "Design Approaches for Soil-Structure Interaction," by A.S. Veletsos, A.M. Prasad and Y. Tang, 12/30/88.

NCEER-88-0032 "A Re-evaluation of Design Spectra for Seismic Damage Control," by C.J. Turkstra and A.G. Tallin, 11/7/88, (PB89-145221/AS).

NCEER-88-0033 "The Behavior and Design of Noncontact Lap Splices Subjected to Repeated Inelastic Tensile Loading," by V.E. Sagan, P. Gergely and R.N. White, 12/8/88.

NCEER-88-0034 "Seismic Response of Pile Foundations," by S.M. Mamoon, P.K. Banerjee and S. Ahmad, 11/1/88, (PB89-145239/AS).

NCEER-88-0035 "Modeling of R/C Building Structures With Flexible Floor Diaphragms (IDARC2)," by A.M. Reinhorn, S.K. Kunnath and N. Panahshahi, 9/7/88.

NCEER-88-0036 "Solution of the Dam-Reservoir Interaction Problem Using a Combination of FEM, BEM with Particular Integrals, Modal Analysis, and Substructuring," by C-S. Tsai, G.C. Lee and R.L. Ketter, 12/31/88.